The role of wave breaking on the development of wave spectra and bispectra in the surf zone

Utrecht University

Daan Wesselman (3348385)
Utrecht University, Department of Physical Geography
MSc Program: Earth, Surface and Water
July 2013

Abstract

Many countries around the world have a coastal area, which provides them with numerous benefits. To protect this first line of defense, it is relevant to have knowledge about the influence of breaking waves on the development of wave spectra and bispectra in the surf zone. This largely determines whether a coast erodes or accretes. Three contradicting theories about the relation between relative dissipation and frequency exist. The objective of this paper is to carry out some real-scale flume experiments that study the behaviour of waves in the surf zone. In the flume a barrier was placed where waves were breaking significantly. Three cases with different wave and water level properties were performed in order to research the differences. The results are that dissipation does not occur in the lower frequency range (0-0.2 Hz), but only in the higher frequency range (0.2 -0.4 Hz). For this higher frequency range a horizontal relation between relative dissipation and frequency is found, but more research about this is needed.

Contents

1. Introduction

Many countries around the world have a coastal area, which provides them with numerous benefits, like the possibility of a harbour or tourism. Furthermore, it is a natural first line of defense. Therefore knowledge of coastal processes is necessary. More specifically, it is relevant to know if and why a coast erodes or accretes under different circumstances. The properties of wind-driven waves determine for a large part the direction of sediment transport. In addition to the height of the waves, it is in particular their shape (symmetrical, skewed or asymmetrical) that affects transport magnitude and direction.

Considerable research on wave transformation in the intermediate and surf zone has already been performed. Wave spectra and bispectra aid in the study how waves develop in onshore direction, however, the role of wave breaking on spectral and bispectral evolution is still subject of considerable debate, as wave breaking itself is not well understood from a physical viewpoint.

In this report, an overview of existing knowledge on the influence of wave breaking on the cross-shore evolution of power spectra and bispectra is provided. This review is divided into several parts. First, research in the shoaling and surf zone is described, respectively. Then, three contradictory theories are elaborated upon. These theories concern the dependency of breaking-induced dissipation on frequency. The review leads to the identification of knowledge gaps, allowing the main questions for follow-up research.

To answer these main questions, real-scale experiments are performed in the Delta Flume in the Noordoostpolder. These experiments are described in the methods. Then the results are shown and the paper ends with a discussion, where the three theories will be discussed, and a conclusion.

2. Determining wave transformation with wave spectra and bispectra

2.1 Description of waves, wave spectra and bispectra

2.1.1 Wave properties in deep, intermediate and shallow water

Wave shapes in deep, intermediate and shallow water are not the same, as shown in Figure 2.1.1. In deep water waves are symmetrical and in the shoaling zone waves start to 'feel' the bed, so that they become non-linear (first skewed and then asymmetrical).

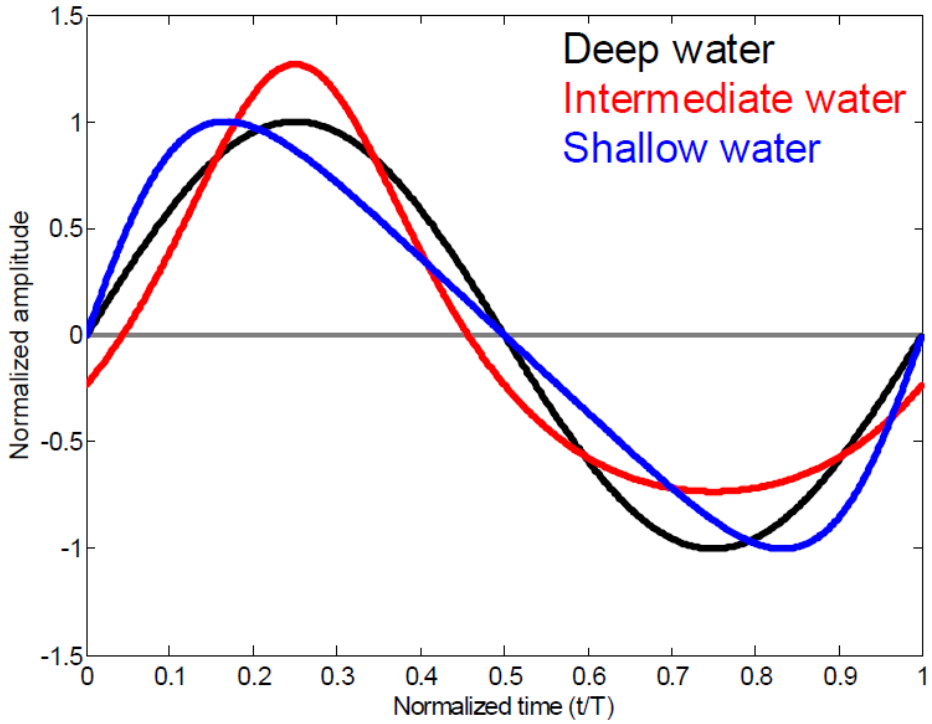

Figure 2.1.1: Three wave types: Symmetrical in deep water with equal crests and troughs, skewed in intermediate water with a short, peaked crest and a broad, flat trough and saw-tooth shaped in shallow water. Source: Ruessink G., Utrecht University, Earth Sciences, Department of Physical Geography, Coastal Morphodynamics.

Linear waves

Waves in deep water have no interaction with the bed, as the orbital motion already damped at this depth. Therefore waves are linear in this zone (black line in Figure 2.1.1), what means an equal crest height and trough depth and an equal crest and trough duration. Moreover, the wave can be mirrored both horizontally and vertically and the wave can be described by one sinus or cosine function.

Non-linear waves – skewness and asymmetry

In the shoaling or intermediate zone and shallow zone, the water depth is small enough for the orbital motion to reach the bed, so that waves become non-linear. Non-linearity can be described by two parameters, namely skewness and asymmetry. Skewed waves have a short, peaked crest and a broad, flat trough (red line in Figure 2.1.1). Properties of these waves are that the crest height/duration is larger/shorter than the trough depth/duration respectively. Moreover, skewed waves deal with wave

transformation relative to the horizontal axis, what means that they can be mirrored in the crest or trough. Asymmetrical waves on the other hand are saw-toothed shaped (blue line in Figure 2.1.1). This means that although crest height is equal to trough depth and crest duration is equal to trough duration, waves cannot be mirrored in the crest or trough. In other words, asymmetrical waves deal with wave transformation relative to the vertical axis. Equations 2.1.1 and 2.1.2 from [Kuznetsov, Saprykina, 2004] give these dimensionless parameters, where η is the sea surface elevation, broken brackets imply averaging over time and H is the Hilbert transform.

$$Sk = \frac{\langle \eta^3 \rangle}{\langle \eta^2 \rangle^{3/2}} \qquad 2.1.1$$

$$As = \frac{\langle H(\eta^3) \rangle}{\langle \eta^2 \rangle^{3/2}} \qquad 2.1.2$$

Equation 2.1.1 shows that if a wave is symmetrical, skewness is zero. However, if a wave is skewed (larger crest height than trough depth), the numerator (power of 3) becomes more important than the denominator (power of 2). Then skewness will have a positive value. Normal values of skewness in the shoaling zone are between 0 and 1 and normally skewness is maximal at the start of the shoaling zone. Equation 2.1.2 is quite similar, but includes the Hilbert transform. One aspect of this parameter is that it makes the result negative instead of positive. Normal values of asymmetry are between -2 and 0. Asymmetry is close to zero at the start of the shoaling zone. The shallower the water becomes, the stronger asymmetry will be.

When waves are non-linear, they cannot be described anymore by one sinus or cosine function, but instead two or more components must be used. These components can be seen as different waves that are bounded or coupled to each other. The phase or biphase between two coupled waves determines the wave shape. If the phase is 0, the waves are skewed, however if the phase is – ½ π the waves are asymmetrical. There is a combination of both when the phase is somewhere in between. More details about the biphase follow in chapter 2.1.3.

2.1.2 Description of a wave spectrum

Wave spectrum in deep water

A wave energy-spectrum separates waves in different frequencies on the x-axis. The long-period waves (small frequencies) are on the left side of the spectrum, while the small-period waves (large frequencies) are on the right side. Per frequency-band, the total energy is calculated and shown on the y-axis of the spectrum. This energy density has a unity of cm^2/Hz and is related to this energy-equation:

$$E = \frac{1}{8} * \rho * g * \Sigma(H^2) \qquad (2.1.3)$$

Here the E states for total energy, ρ is the density of sea water (1025 kg/m^3), g is the gravity acceleration (9,81 m/s^2) and H is the wave height. It becomes clear from equation 2.1.3 that the wave height squared is proportional to the wave energy and thus an important parameter in determining the wave spectrum. In a random wave field in deep water, waves are linear and can be described by one sinus or cosine function. This means that waves have only one frequency and that there is no wave coupling or non-linear energy transfer. In this case, a typical wave spectrum has one central frequency peak with the highest total energy. The spectrum then has more or less a normal distribution or it has the form of a JONSWAP spectrum. An example of such a spectrum is given in Figure 2.1.2. There is a difference between sea and swell waves (Masselink, Hughes, 2003). Sea waves are dominated by the wind and give a broad-banded spectrum, while swell waves develop far offshore and give a narrow-banded spectrum.

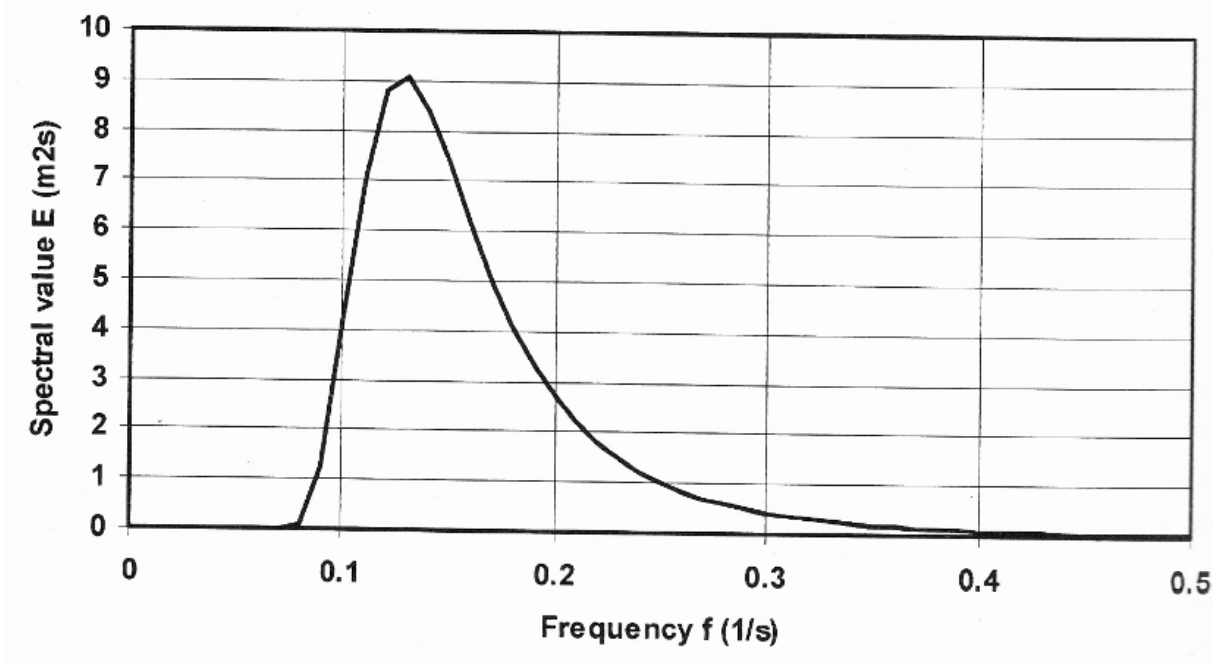

Figure 2.1.2: A JONSWAP spectrum. Source: L.C. van Rijn, Principles of fluid flow and surface water in rivers, estuaries, seas and oceans, Utrecht University, Faculty of Geosciences

Wave spectrum in the shoaling zone

In the shoaling zone however, waves are not linear anymore. This means that waves cannot be described here by one sinus or cosine equation. Instead of this, waves are coupled, as explained in chapter 2.1.1. These wave triads can create higher harmonics (f1 + f2 =f3) or low frequency waves (f1-f2=f4), where f means frequency [Hamm et al, 1993]. These wave triads are also called sum and difference frequencies respectively [Norheim et al, 1997]. Total energy stays constant, as there is no wave breaking yet and bed friction is small. This means that the total energy must be redistributed so that secondary wave energy peaks arise by nonlinear energy transfers. Frequencies that are two, three or four times the initial main frequency peak increase in energy and on the other hand the primary energy peak goes down [Elgar, Guza, 1985]. Now the wave can be described by for example two coupled components of 0.05 and 0.10 Hz respectively. The more onshore waves are, the more non-linear they become. This means that wave coupling increases in onshore direction. Here the focus will be on higher

harmonics and not on low frequency waves. An example of wave spectra were non-linear energy transfers already occurred is given in Figure 2.1.3. This figure shows the development of higher harmonics in shallower water. More information about this figure will be given in chapter 2.2.

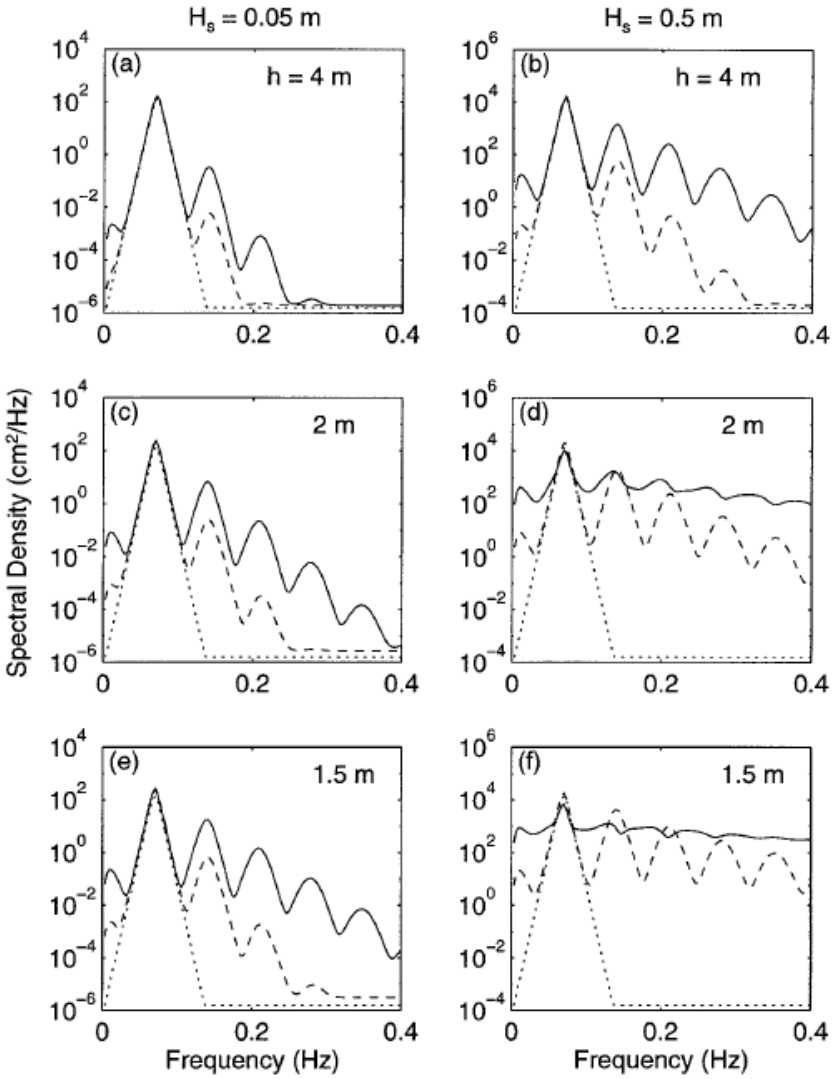

Figure 2.1.3: Simulated wave spectra from [Norheim et al, 1997]. A distinction is made between significant wave height (0.05 and 0.5 meter) and beach slopes. Solid curves have a slope of 1:300 and dashed curves of 1:30. The initial spectrum is indicated with a dotted curve.

2.1.3 Description of a bispectrum

A wave spectrum provides information about the total wave energy per frequency band. Also non-linear transfers are visible, as explained before. The phase between two frequencies however is not shown in wave spectra, also called phase blindness [Collis et al, 1998]. This phase difference determines the shape of the waves (symmetrical, skewed or saw-tooth shaped) and therefore knowledge about it is required. A bispectrum gives this phase information and is therefore an important addition to a wave spectrum in order to analyze wave transformation in the shoaling and surf zone.

Bispectrum

A bispectrum shows the degree of wave coupling between two frequencies. These frequencies are on both axes and the values in the graphs give this degree of coupling (Figure 2.1.4). When these values are positive, there are sum interactions and when these values are negative, there are difference interactions. Especially in a narrow-banded spectrum wave coupling in a bispectrum focusses on the central peak and its higher harmonics, but this will be clearer in chapter 2.2, as well as more details about Figure 2.1.4.

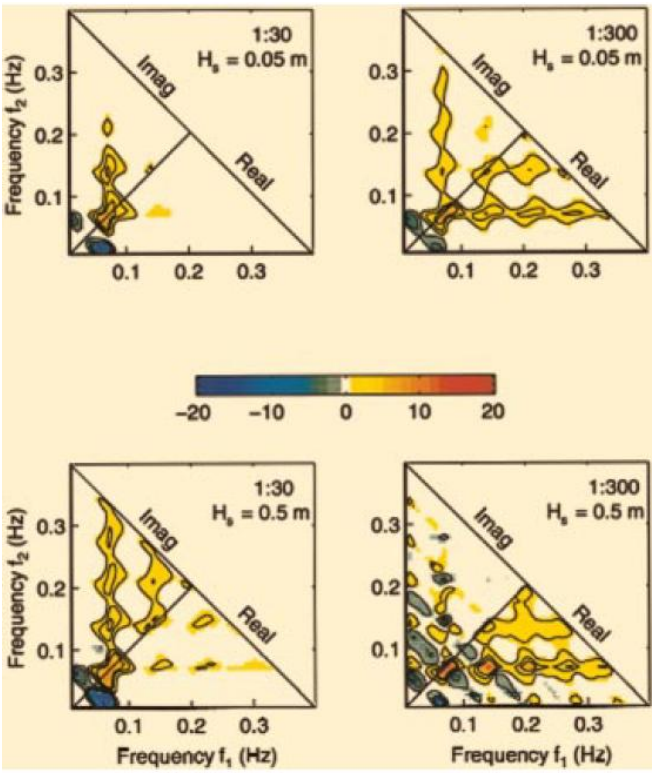

Figure 2.1.4 :Simulated bispectra from [Norheim et al, 1997]. The bispectra are divided in a imaginary (asymmetric waves) and a real part (skewed waves).If the imaginary part is positive, there are sum interactions. Otherwise there are difference interactions. Water depth is 2 meter.

[Norheim et al, 1997] derived equations for the derivates of the wave spectrum E(ω), and the bispectrum B(ω',ω-ω') respectively, where ω means angular frequency:

$$\frac{d}{dx}E(\omega) = -\frac{1}{2h}\frac{dh}{dx}E(\omega) + \frac{3\omega}{2h^{3/2}g^{1/2}} * \int_{-\infty}^{\infty} \mathrm{Im}\{B(\omega', \omega-\omega')\}d\omega' \qquad (2.1.4a)$$

$$\frac{d}{dx}B(\omega', \omega-\omega') = \left(-\frac{3}{4h}\frac{dh}{dx} - i\frac{h^{1/2}\omega'(\omega-\omega')\omega}{2g^{3/2}}\right) * B(\omega', \omega-\omega')$$
$$-i\frac{3}{2h^{3/2}g^{1/2}} * [\omega' E(\omega-\omega')E(\omega) + (\omega-\omega')E(\omega')E(\omega) - \omega E('\omega')E(\omega-\omega')] \qquad (2.1.4b)$$

Here h(x) is the water depth, g the gravity, Im indicates the imaginary part and i is the complex number. In equation 2.1.4a, the first term on the right hand side represents linear shoaling, and the non-linear

transfers are controlled by the integral of the imaginary part of the bispectrum. Also the first term on the right hand side of equation 2.1.4b represents linear shoaling. The energy product terms are dealing with three different interactions (one sum and two difference interactions). When the wave spectrum is known from a model or from observations, the bispectrum equation can be derived:

$$B(\omega', \omega - \omega') = 2[D(\omega', \omega - \omega')E(\omega')E(\omega - \omega') + D(\omega', -\omega) * E(\omega')E(\omega) + D(\omega - \omega', -\omega)E(\omega - \omega')E(\omega)] \quad (2.1.5a)$$

Where D is the coupling coefficient given by

$$D(\omega_1, \omega_2) = \frac{(\omega_1 + \omega_2)^2}{g(\kappa_1 + \kappa_2)\tanh[(\kappa_1 + \kappa_2)h] - (\omega_1 + \omega_2)^2} * \left\{ \frac{\omega_1\omega_2}{g} - \frac{g\kappa_1\kappa_2}{\omega_1\omega_2} - \frac{g}{2(\omega_1 + \omega_2)} * \left(\frac{\kappa_1^2}{\omega_1 \cosh^2(\kappa_1 h)} + \frac{\kappa_2^2}{\omega_2 \cosh^2(\kappa_2 h)} \right) \right\} + \frac{\omega_1^2 + \omega_1\omega_2 + \omega_2^2}{2g} - \frac{g\kappa_1\kappa_2}{2\omega_1\omega_2} \quad (2.1.5b)$$

Here κ is the wave number. The most important thing of equation 2.1.4b (the change in bispectrum) is that it consists of a real and imaginary part. The real part represents skewed waves and the imaginary part represents asymmetrical waves. Following [Elgar, Guza, 1985] and [Norheim et al, 1997], a bispectrum can be split in two parts: The normalized magnitude, called the bicoherence, and the phase between two frequencies, called the biphase.

Bicoherence

[Norheim et al, 1997] found an equation to normalize the bicoherence from the bispectrum equation:

$$b(f_1, f_2) = \frac{B(f_1, f_2)}{[E(f_1)E(f_2)E(f_1 + f_2)]^{1/2}} \quad (2.1.6)$$

The transformation from angular to normal frequency f is performed like this:

$$B(f_1, f_2) = 8\pi^2 B(\omega_1, \omega_2) \quad (2.1.7)$$

This means that the absolute bicoherence value lies between 0 and 1. In a random wave field in deep water, waves are linear without wave coupling. The bicoherence, the magnitude of a bispectrum, is zero when there is no coupling and waves are symmetrical. A value of 1 gives maximal wave coupling. Whether this coupling gives skewed or asymmetric waves is determined by the biphase.

Biphase

[Elgar, Guza, 1985] formulated an equation for the biphase:

$$\beta(\omega_1,\omega_2) = \arctan\left[\frac{\mathrm{Im}\{B(\omega_1,\omega_2)\}}{\mathrm{Re}\{B(\omega_1,\omega_2)\}}\right] \qquad (2.1.8)$$

In other words, the biphase is the ratio between the imaginary and the real part of the bispectrum. In deep water, the biphase between two waves in deep water is unstable and random between π and –π, as waves are not coupled here. Although the phase is random in deep water, it becomes zero when waves start to shoal [Elgar, Guza, 1985]. When the biphase is zero, waves are completely skewed. In onshore direction, the biphase is going towards a final value of – ½ π. When waves are coupled with this phase difference, waves are no longer skewed but asymmetrical. In Figure 2.1.5, an example of the biphase is shown.

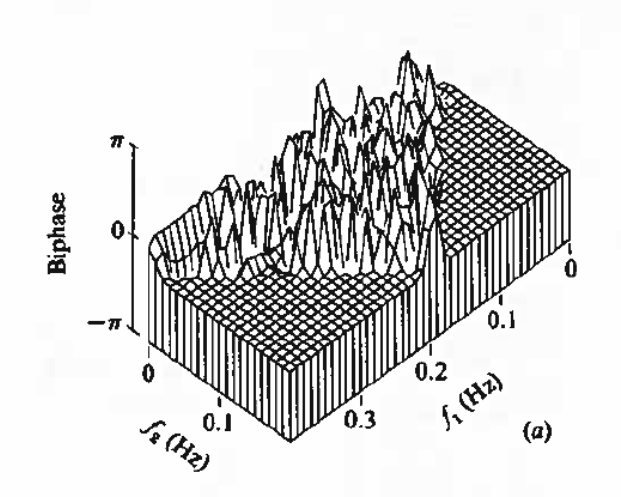

Figure 2.1.5: Biphase for a data set of [Elgar, Guza,1985]. In this 3D-figure, the axis are f_1, f_2 and biphase. Biphase goes from 0 to -1/2 π in the intermediate and shallow zone.

2.2 Wave spectra and bispectra in the shoaling zone

2.2.1 Narrow-banded wave spectra and bispectra

Shoaling zone

[Elgar, Guza,1985] discussed several cases concerning power spectra and bispectra in the field in 1981, where measurements were taken from 9 meter to less than 1 meter depth. The first case was dominated by swell waves with a frequency of 0.06 Hz. This means that this situation was representative of a narrow-banded wave spectrum, without large variations in wave period. The significant wave height was 0.65 meter. At 9 meter depth, where power spectra were assumed to be representative of deep water waves, this 0.06 Hz peak was shown, together with a small peak at the first harmonic (Figure 2.2.1). The first harmonic means that two waves of the primary peak of 0.06 Hz are coupled and added to give a secondary (small) peak of 0.12 Hz.

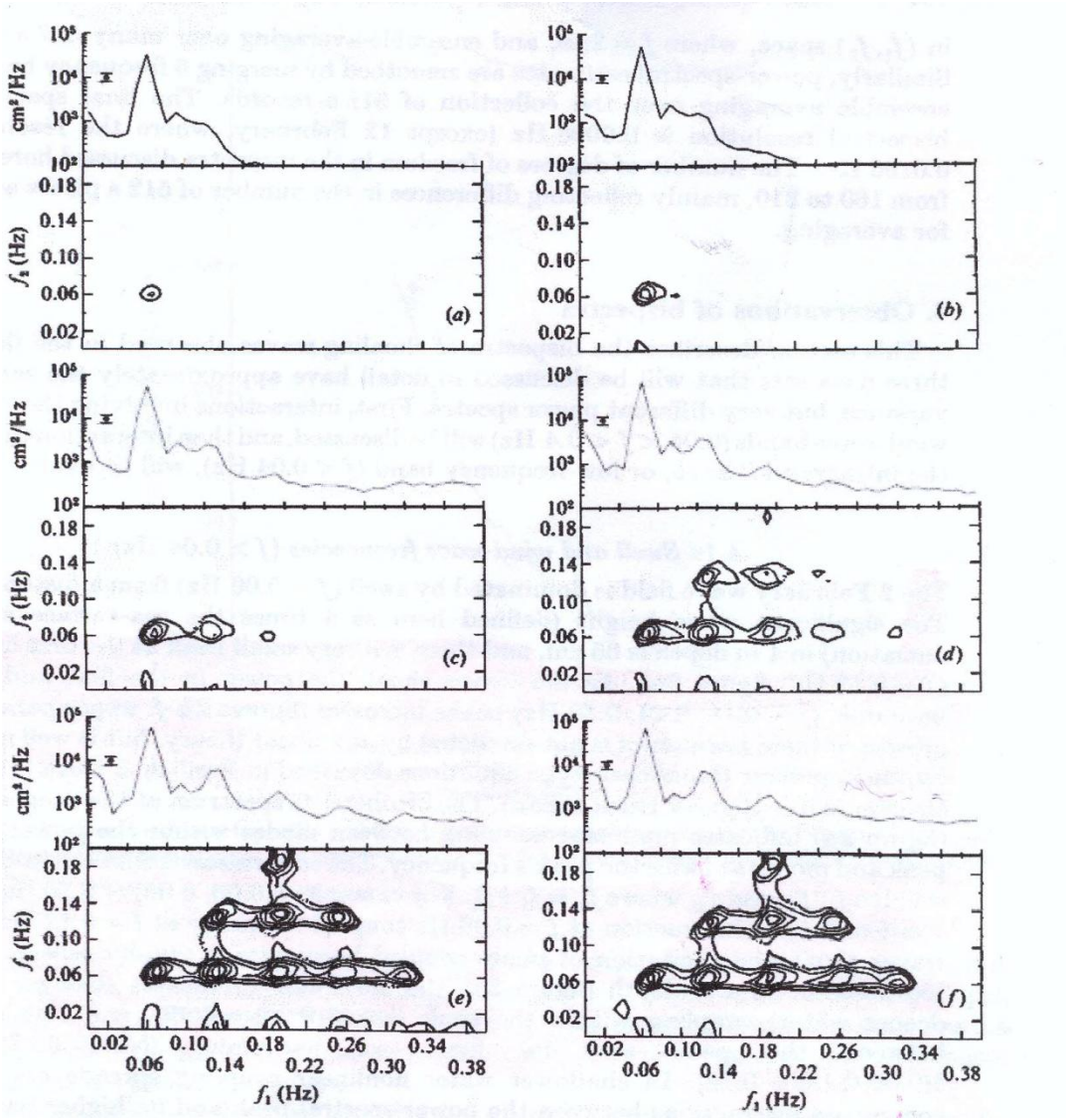

Figure 2.2.1: Wave spectra and bispectra from [Elgar, Guza, 1985]. These results are from a narrow-banded spectrum. Water depths from a to f respectively are 9.0, 6.4, 3.9, 2.7, 2.0 and 1.3 meter.

Apparently wave coupling already started at 9 meter depth. When water depth decreases and waves started shoaling, higher harmonics developed, with frequencies of 0.18, 0.24 and 0.30 Hz, also shown in Figure 2.2.1. These higher harmonics not only existed due to wave triads between the first peak and secondary peaks, but also higher harmonics could be coupled by themselves. For example, 0.12 + 0.12 = 0.24 Hz. In Figure 2.2.1, it is easy to see that the further onshore waves were (so the more they shoal), the more secondary peaks developed at higher harmonics. As total energy should be constant, the primary peak should go down. The bicoherence increased in onshore direction. For example, in 4 meter water depth, the coupling between two 0.06 Hz waves gave a value of 0.49. Also in figure 2.2.1, together with the power spectra, the bispectra are plotted. Also here the same wave coupling is shown as before, with the same higher harmonics. [Elgar, Guza, 1985] made no difference in real and imaginary values, but instead all points were plotted in one way. In 9 meter depth, there is a small spot in the bispectrum that indicates the coupling of the original 0.06 Hz with his first harmonic of 0.12 Hz. Further onshore more wave coupling happened, also with higher harmonics. These wave couplings emerged in a clear way in the bispectra.

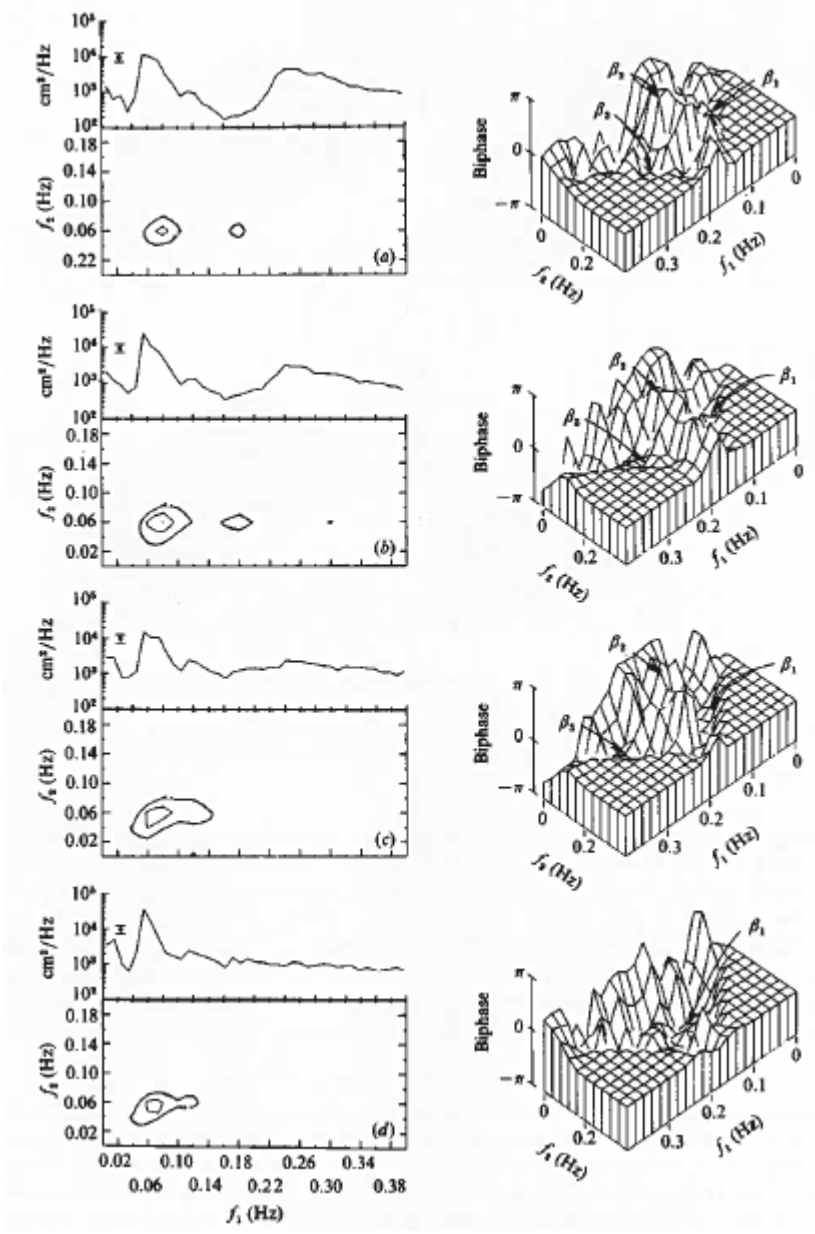

Figure 2.2.2: On the left side wave spectra and bispectra from [Elgar, Guza, 1985].A spectral valley is present between two frequency peaks. In intermediate water the valley is filled by non-linear energy transfers. On the right side the biphase is shown. Water depths form a to d respectively are 3.4, 2.1, 1.4 and 0.8 meter.

In another case, there were two frequency peaks in deep water, namely a narrow swell peak at 0.07 Hz (and also a small one at 0.05 Hz) and a broad sea peak at 0.24 Hz. Between these peaks a spectral valley was visible (Figure 2.2.2). In the intermediate zone, between 1,5 and 2 meter water depth, this valley was filled by two different wave triads: The coupling of two swell waves gave a wave of 0.14 Hz (0.07+0.07) and the coupling of a swell and a sea wave gave a wave of 0.19 Hz (0.24-0.05). At 1.3 meter depth, the spectral valley was almost gone and at 0.8 meter, where some waves were already broken, the valley and the high-frequency peak had the same level.

[Norheim et al, 1997] used a stochastic Boussinesq model to predict spectral evolution of shoaling waves. Directional spreading of waves was neglected, as this causes many side effects that disturb the development of wave spectra. In Figure 2.1.3 again, the simulation results are shown with an initial depth of 6 meter and a spectral peak frequency of 0.07 Hz, whit a narrow-banded spectrum. There were four simulations, with two different significant wave heights (0.05 and 0.5 meter) and two different beach slopes (1:30 and 1:300). All four simulations show the same general patterns as [Elgar, Guza, 1985] in a very clear way, with secondary peaks at harmonic frequencies. As expected, the development of secondary peaks with a significant wave height of 0.5 meter was large compared with a smaller wave height, because shoaling is much larger with larger waves. Furthermore, a gentler beach slope caused more development of secondary peaks than a steep beach slope. For example, with the small wave height and steep slope, only one secondary peak at 4 meter depth was visible (0.14 Hz, what is two times the peak frequency). However, with the large wave height and small slope, also higher harmonics at 0.21, 0.28 and 0.35 were already present at 4 meter depth. In this case, energy transfers filled the valleys between the peaks in shallow water and the spectrum flattened.

In the bispectra of [Norheim et al, 1997], with a real and an imaginary part, the same wave coupling as visible in the wave spectra was shown, at frequencies that are two, three, four or five times the initial peak frequency of 0.07 Hz (Figure 2.1.4). Furthermore, it is clear that the imaginary part (asymmetric waves) dominated with a large beach slope, while the real part (skewed waves) dominated at a gentle beach slope. However, the development of the bispectra in onshore direction was not shown here, as the figure only represents a water depth of 2 meter.

The simulations of power spectra and bispectra were checked with observations by [Norheim et al, 1997]. On this beach, there was a bar with a water depth of about 2.3 meter. The significant wave height was between 0.4 and 0.8 meter. Observations showed the same general patterns as the simulations. At one case, there was a narrow-banded spectrum with a peak frequency of 0.75 Hz. Also here secondary peaks at 0.15, 0.23 and 0.3 Hz were present in shallower water. Both observed and simulated bispectra showed a shift from real (skewed waves) to imaginary values (asymmetric waves) in onshore direction, as shown in Figure2.2.3. This was in line with the theory about non-linear wave transformation in the shoaling zone. However, in very shallow water observations showed a transfer from imaginary to real values, which was absent in the simulated bispectra. This had probably to do with reflected waves generating standing waves. This is not incorporated in the Boussinesq model.

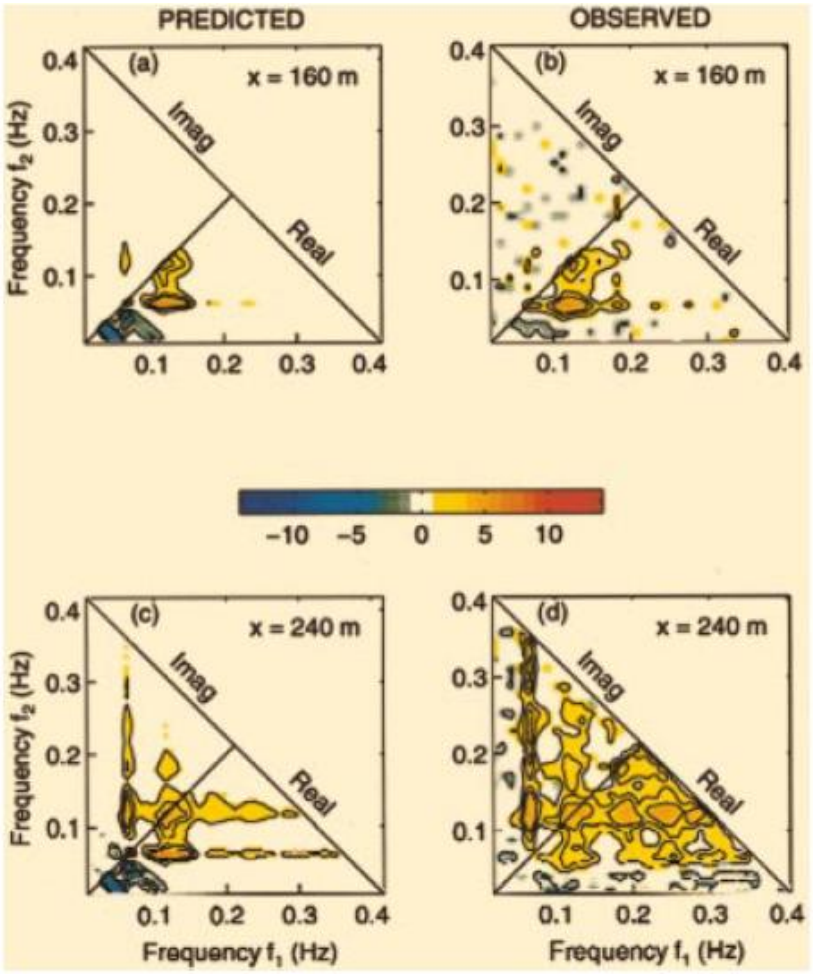

Figure 2.2.3: Comparison of predicted and observed bispectra. Both show an offshore trend from real (skewed waves) to imaginary values (saw-tooth shaped waves). H_s is between 0.4 and 0.8 meter , peak-frequency is 0.75 Hz.

Bars

Moreover, onshore from the bar, when water depth increased again, a shift from imaginary to real values was visible, in other words waves became more skewed again. This was also shown in wave spectra, where the just created higher harmonics were destroyed again and changed in lower frequencies. In other words, when water depth increased after a bar, the opposite effect occurred. This was also noted by [Beji, Battjes, 1993]. They did monochromatic wave experiments in a flume with long waves of 0.4 Hz and short waves of 1 Hz (see also chapter 2.3 about the role of breaking waves). In the flume, a bar was created with an increasing water depth after this bar. The long waves started to form higher harmonics very rapidly. Because of this, a dispersive tail of waves with a higher frequency was created. This wave tail could be seen as free waves, so that they moved independently from the primary waves. Due to this the phase lag between the primary and dispersive tail waves was increasing above the bar. When water depth was increasing again after the bar, de-shoaling occurred and the dispersive tail waves decomposed into several waves with smaller frequency and wave height. In the end, the narrow-banded spectrum was changed in a broad-banded spectrum after passing a bar. For short waves of 1 Hz, a dispersive tail was not visible, as the symmetry was much more conserved here, so also the transformation into a broad-banded spectrum after the bar was not happening.

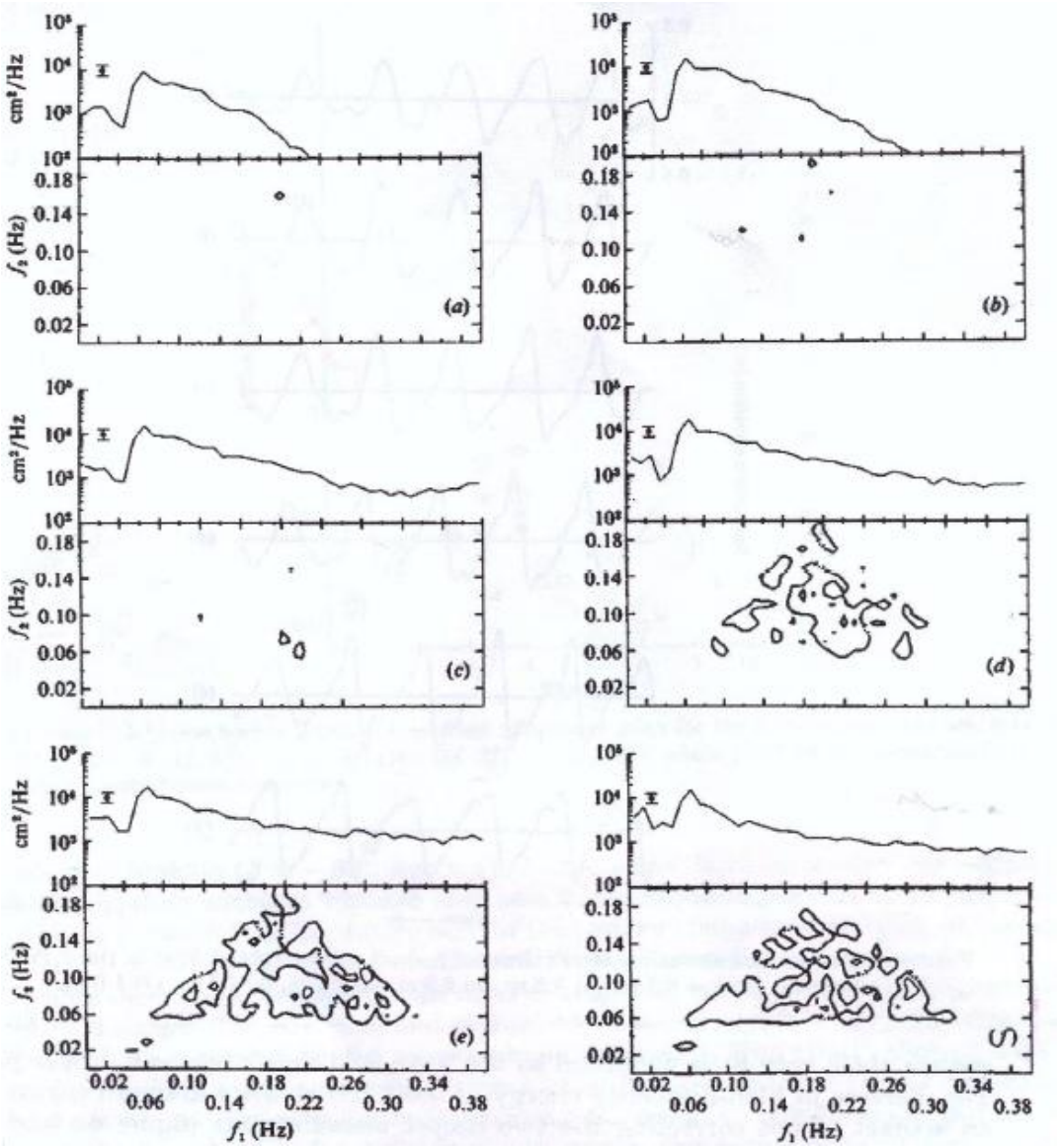

Figure 2.2.4: Wave spectra and bispectra from [Elgar, Guza, 1985]. These results are from a broad-banded spectrum. Wave coupling is less strong here as in figure 2.1.1. Water depths from a to f respectively are 8.7, 6.0, 3.5, 2.2, 1.6 and 0.9 meter.

2.2.2 Broad-banded wave spectra and bispectra

In the third case, [Elgar, Guza, 1985] found some different circumstances. The significant wave height again was 0.65 meter. However, this time there was no narrow-banded swell spectrum, but there were broad-banded sea waves, with more variation in frequency (Figure 2.2.4). As a result, the evolution of secondary energy peaks was less than at the first case. The reason is that there were more different frequencies, so that wave coupling was not concentrated anymore on a few secondary peaks. Instead of this, there was a general increase in higher frequencies. This was also visible in the bicoherence, with a average value of only 0.15 in 0.9 meter water depth. Also the bispectra showed less clear wave coupling. There was wave coupling, but with many different frequency pairs. If Figure 2.2.4 is compared with Figure 2.2.1 (narrow-banded spectrum), it becomes more clear that a broad-banded spectrum gives a bispectrum with less clear wave coupling. However, wave transformation was still the same, with symmetrical, skewed and asymmetrical waves. Therefore the biphase should logically evolve in the same way. This was also visible in the results, with a biphase of zero when waves were skewed and a biphase of $-\frac{1}{2}\pi$ when waves were asymmetrical. The difference was that in a narrow-banded spectrum the

bispectrum was developed with only a few wave triads, while in a broad-banded spectrum it was developed by a many different wave pairs.

Also [Norheim et al, 1997] simulated a test with a broad-banded spectrum. They found a weaker evolution of higher harmonics as well. Secondary peaks were not created, but instead a general increase of the higher frequencies developed, as shown in figure 2.2.5. For the small significant wave height of 0.05 meter, only a very small spectral increase was visible. For the wave height of 0.5 meter, the spectral increase was much larger. Just as with the narrow-banded simulations, spectral flattening occurred in shallow water of 1.5 meter. Also broad-banded spectra were compared with observations, and again the results were almost the same, with a general increase of the spectrum instead of growth of secondary peaks.

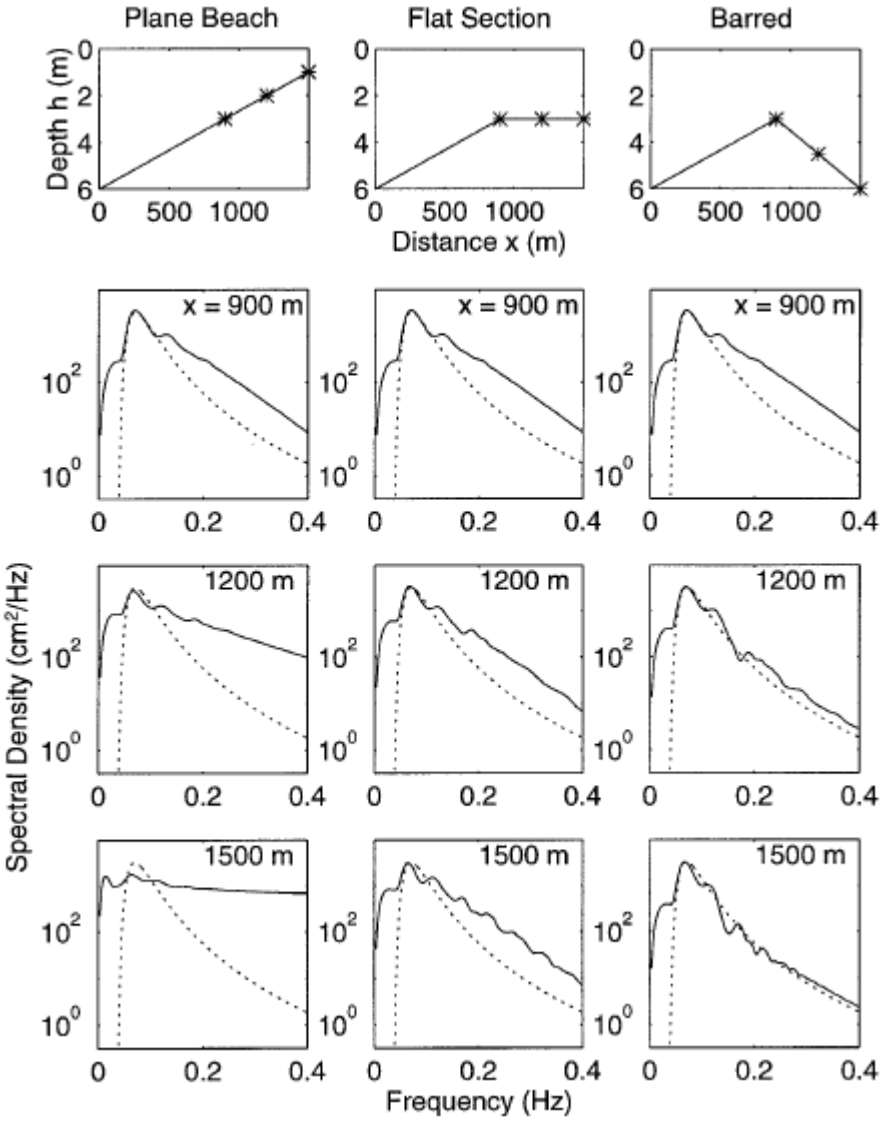

Figure 2.2.5: A broad-banded spectrum from [Norheim et al, 1997]. Secondary peaks are not developing. Instead, a general increase of higher frequencies occurs.

2.3 Wave spectra and bispectra in the surf zone

2.3.1 Introduction

Until now, only wave spectra before the breaking zone were described, because information about the influence of wave breaking on wave spectra was lacking for a long time. The change of the spectra in the shoaling zone is quite clear, and all experiments and models give the same trends. In this section, research on the influence of wave breaking will be described. There are three main theories about how dissipation affects a wave spectrum. These theories will be explained, and the differences will be outlined.

2.3.2 Theory 1: Relative dissipation depends on frequency squared

The first theory is that the dissipation rate increases with increasing frequency, where dissipation is proportional to frequency squared.[Elgar et al, 1997] were one the first to look at the role of wave breaking on nonlinear energy transfers. Wave reflection could be neglected during energetic swell conditions, as nonlinear energy transfers and dissipation were the dominant factors then. They did not research directly the influence of breaking-induced dissipation on the shape of the wave spectrum, but they found a rough relationship between frequency and dissipation. It was admitted that the underlying dynamics were not known yet and that there were some differences between modeled and observed data. However, the relationship between dissipation and frequency was clear (Figure 2.3.1).

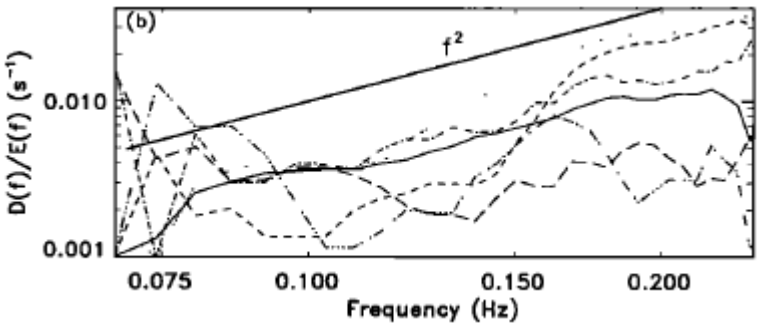

Figure 2.3.1: Breaking-induced dissipation versus frequency from [Elgar et al, 1997]. It can be said roughly that dissipation is proportional to frequency squared.

2.3.3 Theory 2: Relative dissipation is the same for the whole spectrum

The second theory states that breaking is only a secondary process in the transformation of non-linear waves. The total amount of energy is decreasing due to dissipation, but the relative decrease in energy of different frequencies is the same throughout the whole spectrum. [Beji, Battjes, 1993] carried out experiments in a flume with a length of 37.7 meter and a width of 0.8 meter, to research the role of wave breaking on wave transformations. They researched three different wave conditions: non-breaking waves, spilling and plunging breakers. In all three cases, both long waves (0.4 Hz) and short waves (1.0 Hz) were performed. Furthermore, monochromatic waves, a JONSWAP spectrum and a hand-made very narrow-banded spectrum were used for all cases. The monochromatic waves were already mentioned in chapter 2.2.1. For the long waves, higher significant wave heights were used: 4.1, 5.9 and 6.9 cm instead of 2.9, 4.4 and 5.4 cm. This was done in order to keep the nonlinearity parameter, what is the ratio of amplitude and water depth, the same for both long and short waves.

In Figure 2.3.2, the three cases for the very narrow-banded spectrum and long waves at different places in the flume are shown. Station 8 is placed after the bar, where water-depth was increasing again. It is clear that the three wave spectra hardly differ in shape. Secondary peaks are visible at the same position, whether wave breaking occurred or not. Also when a JONSWAP spectrum was used, as is shown in Figure 2.3.3 (where the energy for breaking and non-breaking waves on the y-axis is normalized), breaking waves did not change the shape of the spectrum. However, [Beji, Battjes, 1993] ended with the fact that this was only a start and more research about the role of wave breaking on wave spectra must be done. Important to note is that this is not in line with the conclusion of [Elgar et al, 1997], who said that dissipation depends on frequency squared, while [Beji, Battjes, 1993] stated that the change in the shape of the spectrum is independent of frequency.

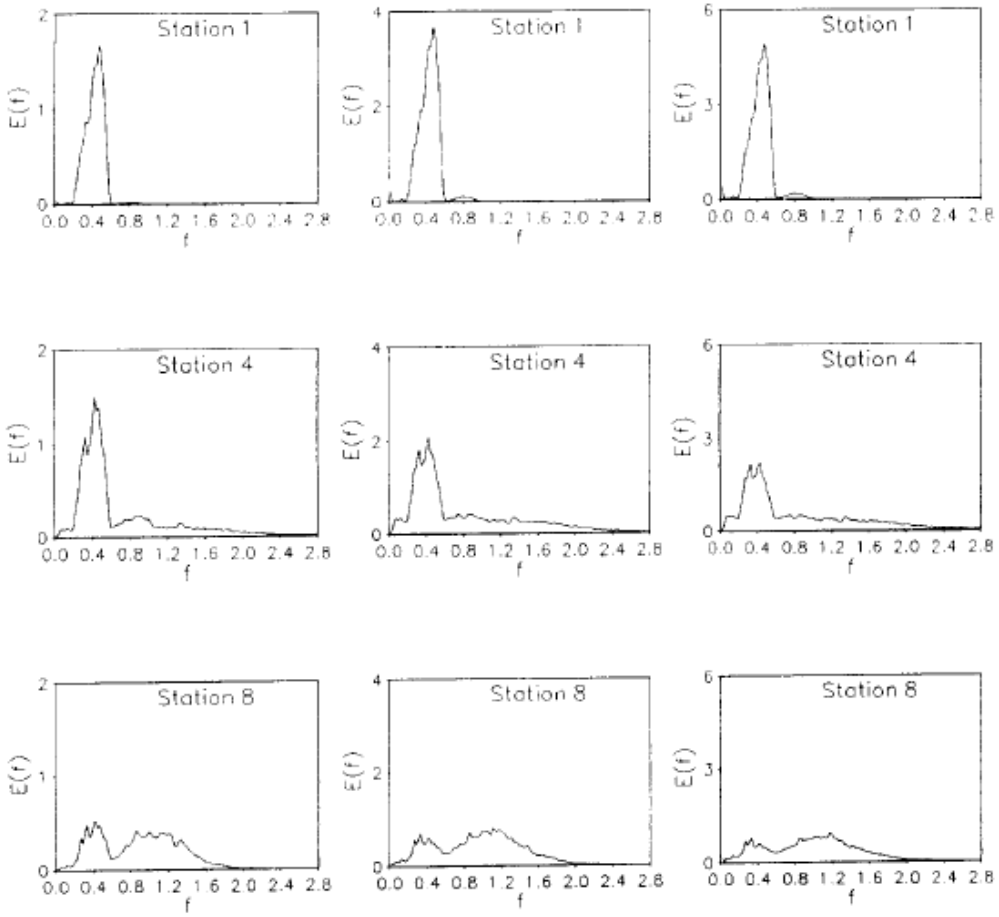

Figure 2.3.2: Wave spectra from [Beji, Battjes, 1993] using a very narrow-banded spectrum. There are non-breakers (left), spilling breakers (middle) and plunging breakers (right). The shape for all three of them is the same.

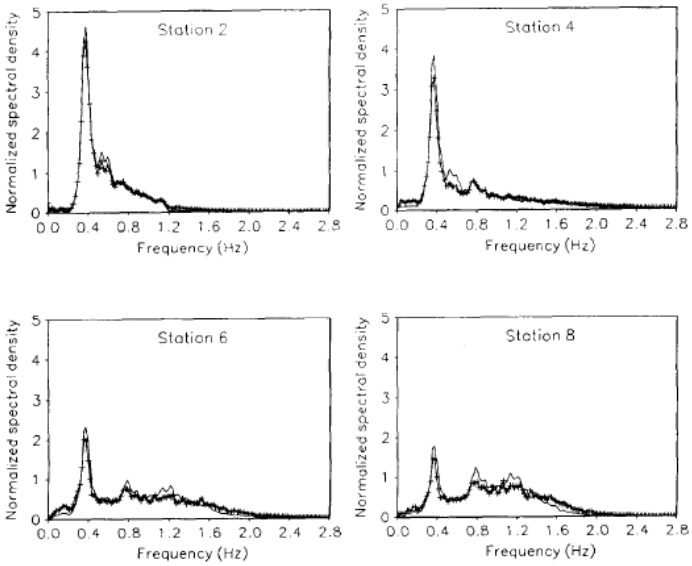

Figure 2.3.3: Wave spectra from [Beji, Battjes, 1993] using a JONSWAP spectrum. Also here are non-breakers (_) and plunging breakers (+). Also here the shape remains the same.

[Eldeberky, Battjes, 1996] developed a model that includes this theory 2. They created a Bousinesq model that included breaking-induced dissipation. The results of this model are compared with experiments, such as the experiment of [Beji, Battjes, 1993] as described before. This model showed the same trend. The amplitude of the wave spectra changed when waves break, but the spectral shape remained the same. Especially for lower frequency the model gave good predictions. [Eldeberky, Battjes, 1996] admitted that a large part is not known yet about wave breaking.

2.3.4 Combination of both theory 1 and 2 – dumping coefficient

[Kuznetsov, Saprykina, 2004] recognized the difference between both theories and stated that models are always based on one of them. Therefore they researched in what situations which theory can be used best. Therefore a dumping coefficient α_n is introduced, which is the rate of energy dissipation during wave breaking for all frequencies. Following theory 2, this dumping coefficient should be uniform for all frequencies, while theory 1 states that this α_n is dependent on frequency squared. The dumping coefficient can be determined with this empirical equation:

$$\frac{dA_p}{dx} = -\beta_2 \frac{h_x}{h} A_p - i2g(F_p^+ + F_p^-) - \alpha_n A_p \qquad (2.7)$$

The left part is the change of the wave amplitude in onshore direction. The first term on the right side is the increase of amplitude in shallow water (shoaling), where β_2 is a coefficient that depends on the local water depth h, the bed slope h_x and the space variations in the wave numbers, so this coefficient includes shoaling. It is not clear why there is a minus sign before this term, maybe β_2 is negative. The second term represents nonlinear triad interactions. The different parameters of this term are not explained. The last term is the breaking-induced dissipation, where the dumping coefficient is included. In this term the dumping coefficient represents the dissipation. There is a minus sign, because the larger the dumping coefficient, the more wave-induced dissipation, the smaller the change of A_p in onshore direction. Using differential techniques this equation can be solved. For calculating this dumping

coefficient, two different field experiments were used, comparable with other field work, so that different conditions were included (like sea-swell waves, different types of wave breaking and different significant wave heights). The most important difference between the two field works was the mean bed slope (0.027 versus 0.014)

Results show the same patterns as before, with secondary peaks in shallower water due to wave transformation. More interesting is the development of the dumping coefficient in the surf zone, as shown in Figure 2.3.4. In the outer surf zone, where the larger waves start to break, the dumping coefficient is more or less uniform. This is in line with theory 2, so that the shape of the spectrum will not change (Figures 2.3.4.e and g). However, in the inner surf zone it is different. Here the dumping coefficient increases exponentially with increasing frequency, as shown in Figures 2.3.4.d and f. It must be noted that in the inner surf zone there is sometimes also other behaviour of α_n, but the increasing trend with increasing frequency still exists. So the conclusion of [Kuznetsov, Saprykina, 2004] is that the role of dissipation on the change in wave spectra in the surf zone does not depend on the type of wave breaking, but on where wave breaking takes place, and that both theories are partly right.

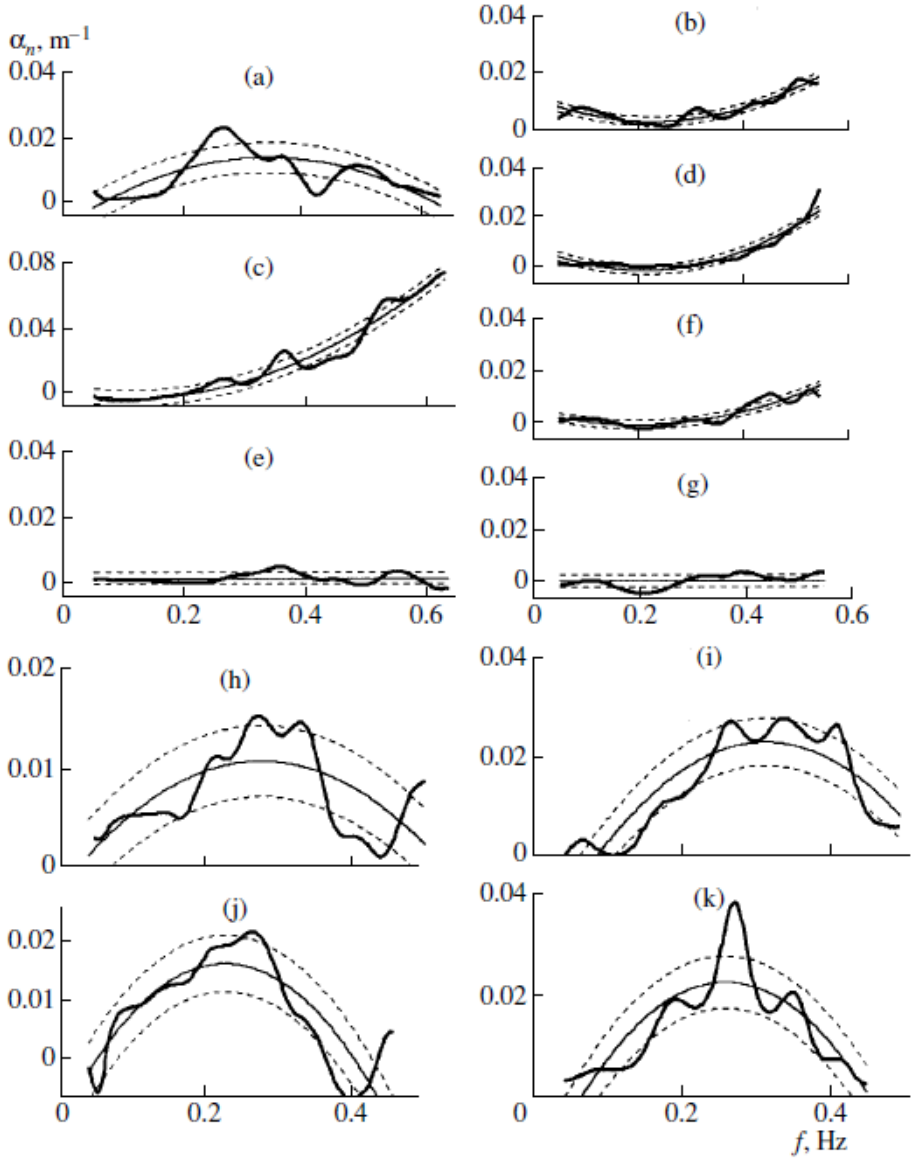

Figure 2.3.4: The behaviour of the dumping coefficient [Kuznetsov, Saprykina, 2004]. The thick line is the relative dumping coefficient, as function of frequency. E and g are in the outer surf zone, d and f are in the inner surf zone.

[Kuznetsov, Saprykina, 2004] tried to make a connection between the frequency-dissipation relation and the shape of the waves. Therefore the degree of skewness and asymmetry is calculated. They conclude that this relation has mainly to do with the degree of asymmetry of the waves. When the asymmetry is relatively weak, the dumping coefficient is uniform, while when this asymmetry increases and waves become saw-tooth shaped, the dumping coefficient becomes proportional to frequency squared. No such a relation is found for the degree of skewness. Also the role of the bed slope is researched, and a relation is found that smaller bed slopes have frequency-dependent types of dissipation, whereas larger bed slopes have a uniform dumping coefficient.

2.3.5 Theory 3 – Dissipation only occurs at higher frequencies

Theory 3 states that breaking-induced dissipation only occurs at higher frequencies and not at the primary frequency. [Herbers et al, 2000] looked at the role of dissipation due to wave breaking on the transformation of wave spectra somewhat different. They created a formula including the cross-shore gradient of the energy flux $F_x(f)$, a nonlinear source term $S_{nl}(f)$ and a breaking-induced dissipation term $S_{ds}(f)$:

$$F_x(f) = S_{nl}(f) + S_{ds}(f) \tag{2.8}$$

F_x is calculated with this equation:

$$F_x = c_g(f)\rho g E(f) \tag{2.9}$$

Where c_g is the group speed, ρ is the density of seawater, g is gravity and E(f) is the surface elevation spectrum. The group speed is calculated with $c_g=(gh)^{0,5}$. The non-linear source term depends on transfers of energy by wave triads. If wave energy for a specific frequency goes down, S_{nl} will be negative, and vice versa. $S_{nl}(f)$ is calculated like this:

$$S_{nl}(f) = \mathrm{Im}\left\{\frac{3\pi f}{h}\rho g\left(\int_0^f df' B(f', f-f') - 2\int_0^\infty df' B(f', f)\right)\right\} \tag{2.10}$$

Im means again the imaginary part, and B is the bispectrum. The dissipation term is known if the other two terms are calculated. Also [Herbers et al, 2000] did field experiments in order to research power spectra. The bed contained a bar. However, except calculating power spectra or bispectra, which were similar to the ones as described before, also graphs where the energy flux gradient and the nonlinear source term are plotted were made. A distinction is made between two cases with different wave conditions in order to compare the role of dissipation.

Case 1 was characterized by a narrow-banded spectrum with a swell peak and a significant wave height of 0.4 meter. Waves were not breaking significantly, so this situation was comparable with earlier field work. In Figure 2.3.5, F_x and S_{nl} are plotted. Power spectra are not shown, because they show the same general patterns as before, with more secondary peaks in the onshore direction. From Figure 2.3.5 it becomes clear that the non-linear source term is largely negative nearby the primary peak of 0.07 Hz in shallow water. However, around the higher harmonics of 0.14 and 0.21 Hz this term is positive. This is in

line with power spectra, where the primary peak goes down and higher harmonics rise. The positive and negative values more or less balance each other, which says that total energy is conserved. This is expected, as there is almost no wave breaking.

Case 2 (Figure 2.3.6) is more interesting because these data were measured during storm conditions with a significant wave height of 2.2 meter and a primary peak of 0.125 Hz. These conditions caused significant wave breaking at and seaward from the bar. The nonlinear source term shows the same trend as in case 1, with negative values around the primary peak and positive values at higher frequencies, showing an energy transfer from low to high frequency. However, due to the much larger wave height, the negative value of S_{nl} around the primary peak is much more negative as in case 1. The energy transfer is maximal above the sand bar. When the plotted energy flux gradient F_x is analyzed, it becomes clear that in the low-frequency range (around the primary peak) it has about the same magnitude as S_{nl}. This proves that the decrease of energy around the spectral peak is mainly due to nonlinear energy transfers, and not due to breaking-induced dissipation, despite the storm conditions. Around the higher frequencies, the story is different. Here the two terms do not match. Where S_{nl} is positive due to wave triads, F_x is very close to zero, as is shown in Figure 2.3.6. The difference must be dissipation through the breaking waves. [Herbers et al, 2000] suggest that energy in the higher frequencies cannot be absorbed and therefore is dissipated at the same rate as it is transferred. They give as possible reason for this that interactions in this high-frequency tail are not-resonant, in contrast to wave triads. However, more research about this is needed. Most important is that this third theory differs from the other two, because it states that there is no dissipation at the primary frequency at all.

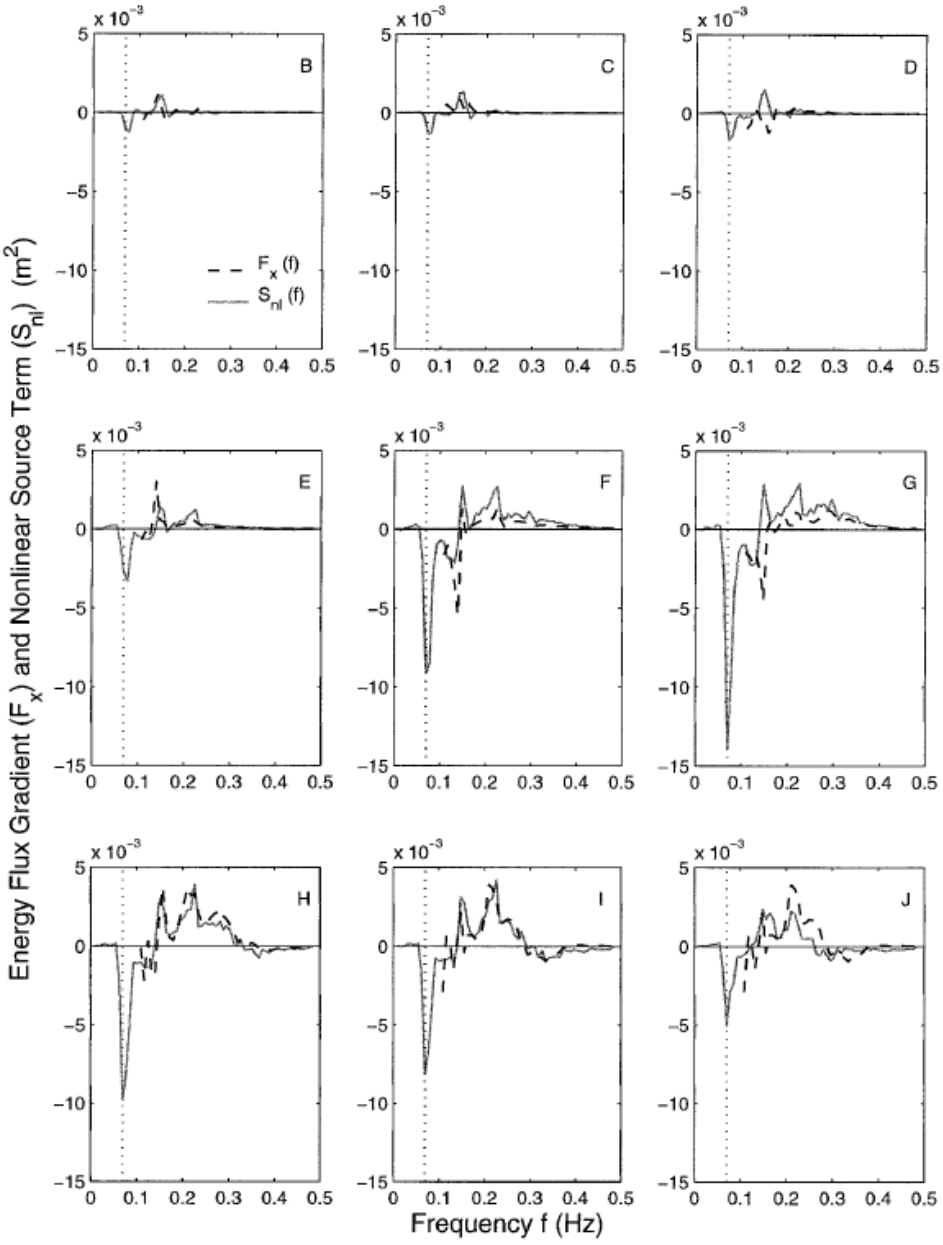

Figure 2.3.5: Comparison of the energy flux gradient (F_x)(f)), dashed curve, and the nonlinear source term S_{nl}(f), solid curve in the first case [Herbers et al, 2000]. Total energy is conserved, as there is no wave breaking.

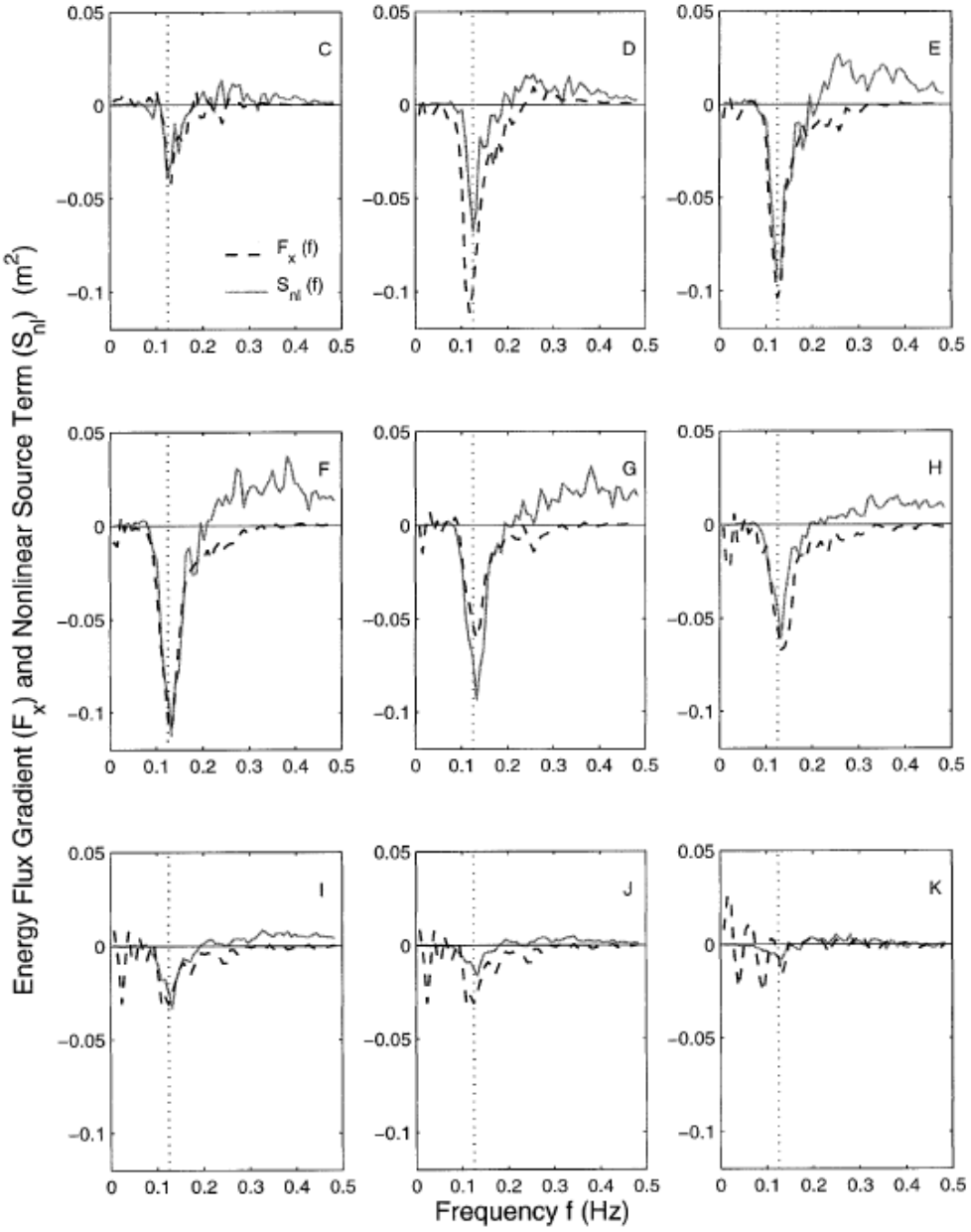

Figure 2.3.6: Comparison of the energy flux gradient (F_x)(f)), dashed curve, and the nonlinear source term S_{nl}(f), solid curve in the second case [Herbers et al, 2000]. Only in a higher frequency range there is energy dissipation.

3. Aim of the flume experiments – research questions

The first part of the literature review described the properties of wave spectra and bispectra in the shoaling zone, prior to wave breaking. Wave triads create higher harmonics and the primary peak goes down in energy. The phase between two coupled waves changes from zero to – ½ π in very shallow water. This causes wave transformation, where waves firstly change into skewed waves and after that become asymmetrical or saw-tooth shaped.

When waves reach the surf zone, where waves start to break, the spectral/bispectral evolution becomes more complicated. For a long time, there was no knowledge at all about the influence of breaking-induced dissipation on wave spectra and wave transformation. In a later stadium a few attempts were done with experiments, field work and models to get a better understanding of this process. However, researchers do still not agree at all points, especially about the dependency of dissipation on frequency. As shown in the literature research, three main theories exist, namely that dissipation is proportional to frequency squared, that dissipation is independent of frequency and that dissipation only occurs at higher frequencies, so that spectral decrease around the primary peak only comes from wave triads. Until now, no clear answer is given for this problem. Furthermore, the authors of the papers in which these theories are explained, admit that there are many uncertainties and that underlying processes are poorly understood.

To get a better understanding of this problem, experiments were performed in the Delta Flume in the Noordoostpolder, the Netherlands. Until now, measurements used for researching the influence of breaking waves on wave spectra came from the field or relatively small-scaled experiments. This flume gives the possibility to simulate waves on real scale in a highly controlled environment.

With this in mind, the main research question and the subquestions can be formulated. The main question is:

What is the role of wave breaking on the development of wave spectra and bispectra in the surf zone?

The subquestions are:

- Is the spectral decrease around the primary peak in the surf zone due to dissipation, or only because of wave triads?
- If dissipation is dependent on frequency, what is this relation? Is it proportional to frequency, or is this relation different?
- Can the dissipation-frequency relation be influenced by variation in circumstances like wave height, type of wave-breaking and wave period?

4. Methods

4.1 Wave experiments

Wave experiments were performed in the Delta flume of Deltares in the Noordoostpolder, the Netherlands, in June and July 2012. These experiments were done for the project Barrier Dynamics Experiment II. (BARDEX II). The data of these experiments are used to answer the main question as described in chapter 3.

4.1.1 Flume properties and sand/water conditions

The flume was 240 meter long, 5 meter wide and 7 meter deep, so that waves could be on real scale. The sediment had a D_{10} of 0.3 mm., a D_{50} of 0.5 mm. and a D_{90} of 0.9 mm. In the flume a barrier was constructed that was 4.5 meter high and 5.0 meter wide. The length of the barrier in horizontal direction was 60 meter. Shoreward from this barrier a lagoon was situated. Waves were breaking significantly on this barrier, but the lagoon was not used for this research. In Figure 4.1 a schematic figure of the initial flume setting is shown. It must be noted that due to morphology change the position and form of the barrier changed over time during the experiments. Also the water level H_s was variable.

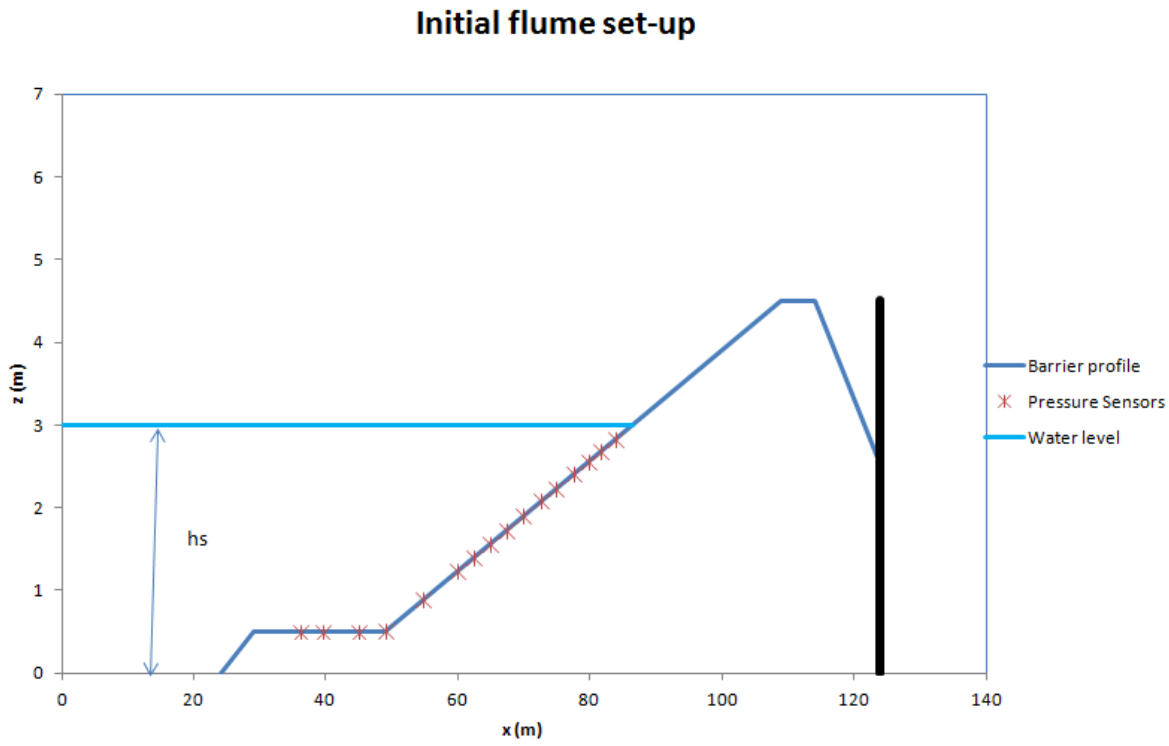

Figure 4.1: A schematic figure of the flume set-up. The barrier is shown, just as the positions of the pressure sensors. Also the mean sea level is indicated with the arrow. Here it is 3 meter, but this was variable with different conditions (see table 4.1).

Several conditions were used with different significant wave heights H_s (from 0.6 to 0.8 meter), periods P (from 4 to 12 seconds) and sea levels h_s (from 2.5 to 3 meter). Within these conditions, several runs varying from 10 minutes to 3 hours were performed. For making bispectra that are trustworthy and detailed, large time series are needed. Therefore several runs of 1 condition were combined to 1 large

run. For this research three cases are outlined, as shown in table 4.1. In this table also the original condition names and runs that are used from BARDEX II are shown. Waves were random with a signal of a JONSWAP spectrum. Waves are assumed to flow in onshore direction. Flow in y-direction is assumed to be zero.

The three cases are chosen, because they differ in significant wave height, period and water level. Case 1 is important, because here the initial bed slope was still intact. Case 2 is chosen to research possible differences in non-linear energy transfers and dissipation due to other wave conditions (smaller wave height, larger period). Case 3 is chosen due to the smaller water level. The wave conditions of case 3 are similar to case 1, so the influence of water level can be researched here.

Case	H_s (m)	P (s)	h_s (m)	Run time (min)	Original condition name	Used runs
1	0.8	8	3	240	A1	6-13
2	0.6	12	3	180	A6	9-13
3	0.8	8	2.5	210	B2	1-6

Table 4.1: Three different cases are used for this research. Also the original condition names and runs from BARDEX II are shown.

4.1.2 Instruments

For this research only pressure sensors were needed, although other instruments were present as well, that measured flow velocity and sediment concentration. 16 pressure sensors were present in total. The positions of them are shown in Figure 4.1. The first four sensors were placed on the initial flat bed and the other 12 were placed on the initial slope of the barrier. Pressure sensors 1, 2 and 3 were on the right wall (in onshore direction) and measured with 20 Hz. Pressure sensors 6, 8, 10 and 12 were placed on a frame on the right wall and measured with 4 Hz. The remaining instruments were OSSI's on the left wall and they measured with 5 Hz. In table 4.2, the x positions of the pressure sensors are shown. For case 2, pressure sensor 16 was not working, just as pressure sensor 10 for case 3. Furthermore, pressure sensors 13-16 were not working during case 3, because they were above the water level. Offshore the distance between the pressure sensors is in the order of 4-6 meter. More onshore, which is the most interesting part (the surf zone), the distance is in the order of 2-2.5 meter. After each run, the bed profile was measured, so that the water level for each instrument was known.

Pr. sensor	**x (m)**	**Pr. sensor**	**x (m)**	**Pr. sensor**	**x (m)**	**Pr. sensor**	**x (m)**
Pr. Sensor 1	36.2	Pr. Sensor 5	54.8	Pr. Sensor 9	67.4	Pr. Sensor 13	77.5
Pr. Sensor 2	39.7	Pr. Sensor 6	59.9	Pr. Sensor 10	70.0	Pr. Sensor 14	79.9
Pr. Sensor 3	45.0	Pr. Sensor 7	62.5	Pr. Sensor 11	72.7	Pr. Sensor 15	81.8
Pr. Sensor 4	49.1	Pr. Sensor 8	65.0	Pr. Sensor 12	74.9	Pr. Sensor 16	83.9

Table 4.2: The x positions of all pressure sensors

4.2 Calculating wave parameters, (bi)spectra and energy flux

For all wave parameters, spectra and bispectra, the sea surface elevation (SSE) is used instead of the pressure. Converting pressure into sea surface elevation requires a correction for the distance between instrument and bed (sometimes several centimeters) and for the air pressure.

4.2.1 Skewness and asymmetry

For calculating skewness and asymmetry, equation 2.1.1 and 2.1.2 are used. As these parameters are based on the SSE, there is one value per instrument for both. They are dimensionless. As explained in chapter 3, skewness is positive between 0 and 1 and asymmetry is negative between -2 and 0. First the skewness and asymmetry for all separated runs are calculated. Then the mean of all runs used for one case is taken.

4.2.2 Wave spectrum

A wave spectrum (Hz versus m^2/Hz) needs a few parameters as input. Firstly the SSE is needed. These data are resampled so that all instruments measurements are changed in 4 Hz. This is done to make it easier to compare all x-positions and to make the calculation time shorter (especially with bispectra). Moreover, the SSE is detrended. Then the data are divided in blocks, using 50% overlap. For the wave spectra, a block length of 3.5 minutes is chosen. The total number of samples in one block is then 3.5*60*4 is 840. If this length is larger, there are fewer blocks. It is possible then that the results are statistically not reliable anymore (larger confidence interval, b95, and lower degrees of freedom, DOF). However if this length is smaller, the spectra could be not detailed enough. Furthermore, the maximum allowed fraction of measurements of pressure that were not performed (gf) is set at 0.1. If this number in one block is larger, then this block is not taken into account. The b95 and DOF for all three cases are shown in table 4.3

Wave spectra		
Case	b95	DOF
1	0.67-1.66	38
2	0.67-1.66	38
3	0.67-1.66	38

Table 4.3: Confidence interval (b95) and degrees of freedom for making wave spectra for all three cases.

4.2.3 Wave bispectrum

The bispectra (m^3) are calculated with the method of [Norheim et al, 1997]. The bispectrum, bicoherence and biphase are calculated with equations 2.1.5, 2.1.6 and 2.1.7 respectively. Again the resampled and detrended SSE must be inputted, just as the sampling frequency of 4 Hz. For the bispectra, there is chosen for a block length of 7 minutes (1680 samples) in order to get more detailed results. The number of frequency bands is set at 3 and gf is again 0.1. The b95 and DOF of the bispectra for all three cases are shown in table 4.4.

Wave bispectra		
Case	b95	DOF
1	0.12	394
2	0.15	318
3	0.11	420

Table 4.4: Confidence interval (b95) and degrees of freedom for making wave bispectra for all three cases.

4.2.4 Energy flux and non-linear wave energy transfers

The energy flux and the transfer of non-linear wave energy (m^2) are calculated using the method of [Herbers et al, 2000]. Equation 2.9 calculates the energy flux (F_x) and needs the group speed, the density of water (in this case 1000 instead of 1025 kg/m^3) and the spectrum. The flux is the gradient of energy as

function of frequency between two x-positions. Therefore the flux is calculated at positions between two instruments. Equation 2.10 calculates the non-linear source term (S_{nl}) and needs the imaginary part of the bispectrum. In order to compare, S_{nl} must also be known between two instruments. This is done with equation 4.1 [Herbers et al, 2000]. So for both parameters, only 15 positions instead of 16 are left. They are both functions of frequency.

$$S_{nl} = \frac{3\pi f}{2}\,\mathrm{Im}\left\{\int_0^f df'\left(\frac{B_1(f', f-f')}{h_1} + \frac{B_2(f', f-f')}{h_2}\right) - 2\int_o^{f_{max}-f} df'\left(\frac{B_1(f', f)}{h_1} + \frac{B_2(f', f)}{h_2}\right)\right\} \quad 4.1$$

S_{nl} is the non-linear source term, B_1 and B_2 are the bispectra at two consecutive instruments and the same holds for the depths h_1 and h_2.

4.2.5 Relative dissipation

The dissipation as a function of frequency (m^2) is equal to the difference of S_{nl} and F_x (equation 2.8). This dissipation then is divided by the spectra energy in order to get the relative dissipation (s^{-1}). The wave spectra must also be between two instruments. For this reason two spectra of two consecutive pressure sensors are averaged.

4.3 Coherence-squared and reflection

In Figure 4.2 the coherence-squared is shown for all three cases. The coherence squared gives a relation between two consecutive pressure sensors. When there is a lot of noise, the relation between two sensors is less and when there is no noise, the coherence-squared is 1. It is necessary to know this value, because in the results the energy flux gradient is related to two different pressure sensors. Case 1 gives coh2 values that are very close to 1. However, from 0.30 Hz it is going down, which means that the results can only be checked until 0.30 Hz. At higher frequencies, there is too much noise then to calculate the energy flux between two pressure sensors. Case 2 shows already lower values (around 0.9), so the results from this case are less trustworthy than case 1. Case 3 shows even lower values (0.7 at 0.2 Hz).

Figure 4.3 shows the reflection as function of frequency for case 1, 2 and 3. The reflection is calculated using the least-squares method. This method requires a simultaneous measurement of the waves at three different positions in the flume in reasonable proximity to each other [Mansard, Funke, 1980]. The first three pressure sensors, which are placed at the offshore horizontal bed, are used for this. The reflection is a possible cause for the decreasing coherence-squared values in case 2 and 3. For case 1, the reflection is quite low for the frequency range 0.1-0.25 Hz (more or less 0.03). In the higher frequency range reflection increases to 0.2-0.4, which is very high. This follows the same trend as the development of the coherence squared. During case 2 there is more reflection as well in the frequency zone 0.1-0.25. In this range the reflection fluctuates between 5 and 10%. This is expected, because due to morphology change the bed has become steeper here, which should cause more reflection. In case 3 the reflection in the frequency range 0.1-0.25 Hz even reaches 15%. These reflection values for case 2 and 3 are higher than the ignored reflection during the experiments of [Elgar, Guza,1985] and [Norheim et al, 1997].

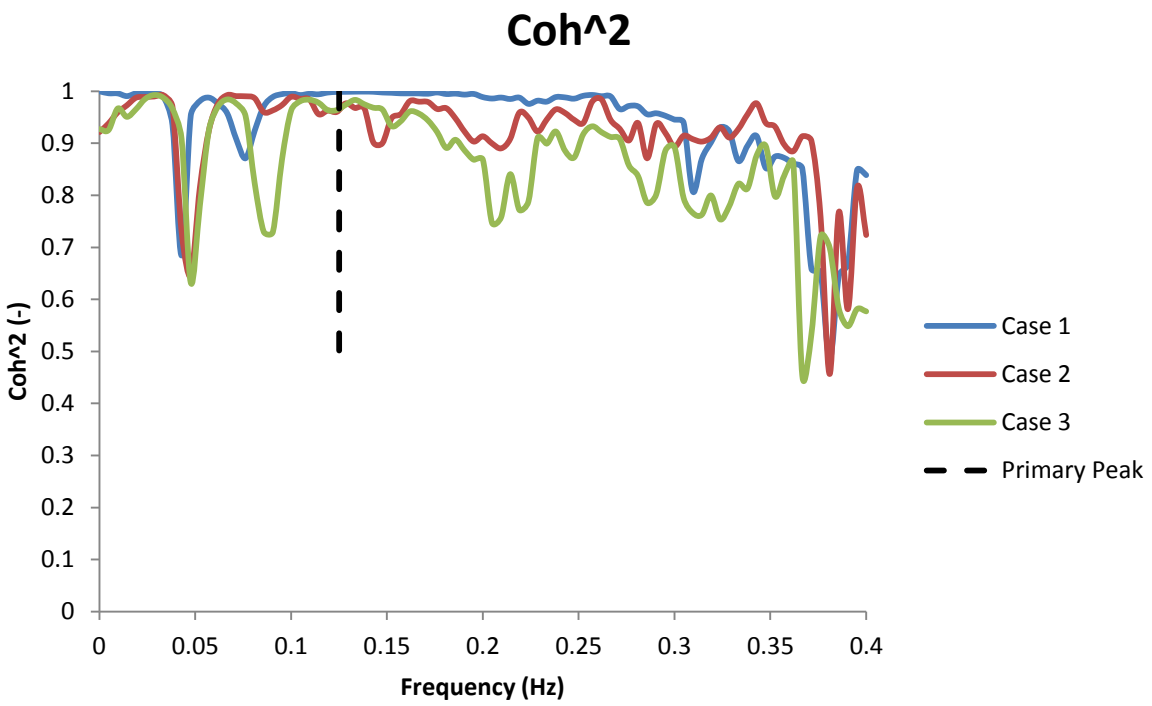

Figure 4.2: Coherence-squared for all three cases. Above 0.30 Hz, the coherence-squared is decreasing. For case 2 and 3, it is already lower in the frequency range 0.15-0.3 Hz.

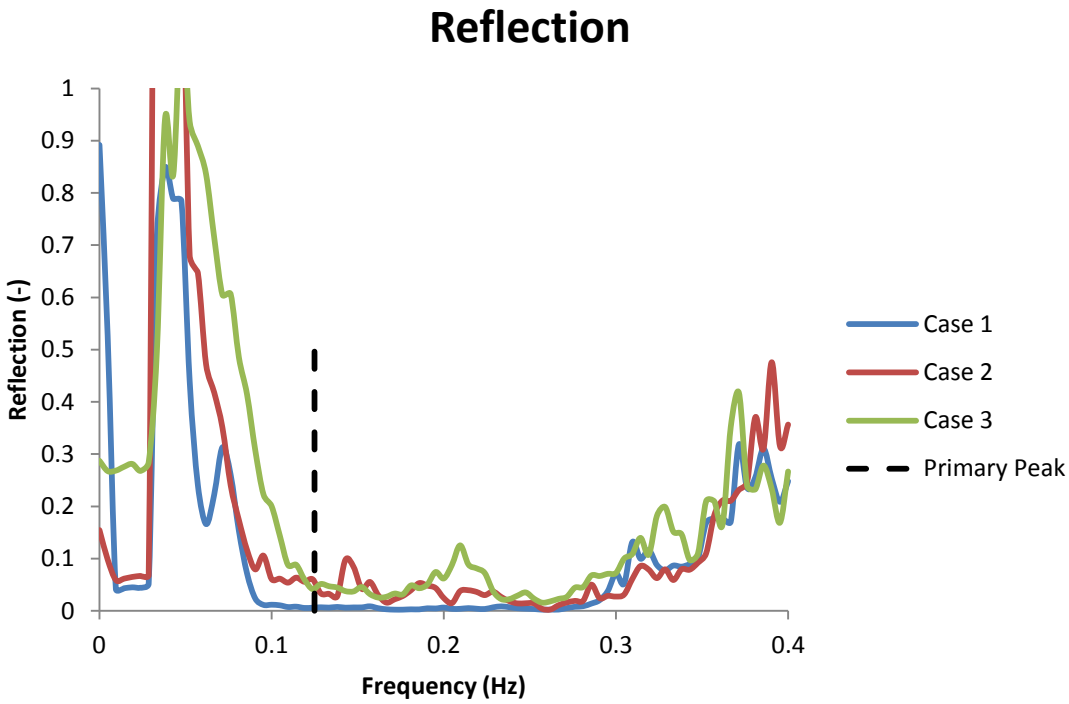

Figure 4.3: Reflection for all three cases. The reflection of case 2 and 3 is clearly higher than for case 1.

The increase of reflection can be explained with the development of the bed due to morphology change (Figure 4.4). Case 1 is the most similar to the initial bed profile. The slope of the barrier is more or less intact, except for some small disturbances. The bed profile of case 2 is already influenced by large morphodynamic changes. Between 45 and 65 meter, the profile is similar to the initial bed, but then the slope becomes steeper until 72 meter, and a small bank is already visible. For case 3, the bed changed even more. At a position of 65 meter the slope is so steep that the sand forms a steep berm. After that the bed becomes flat again. These very steep slopes during case 2 and especially the steep berm of case 3 can cause problems for the wave signal due to reflection, as a very steep slope prevents wave breaking.

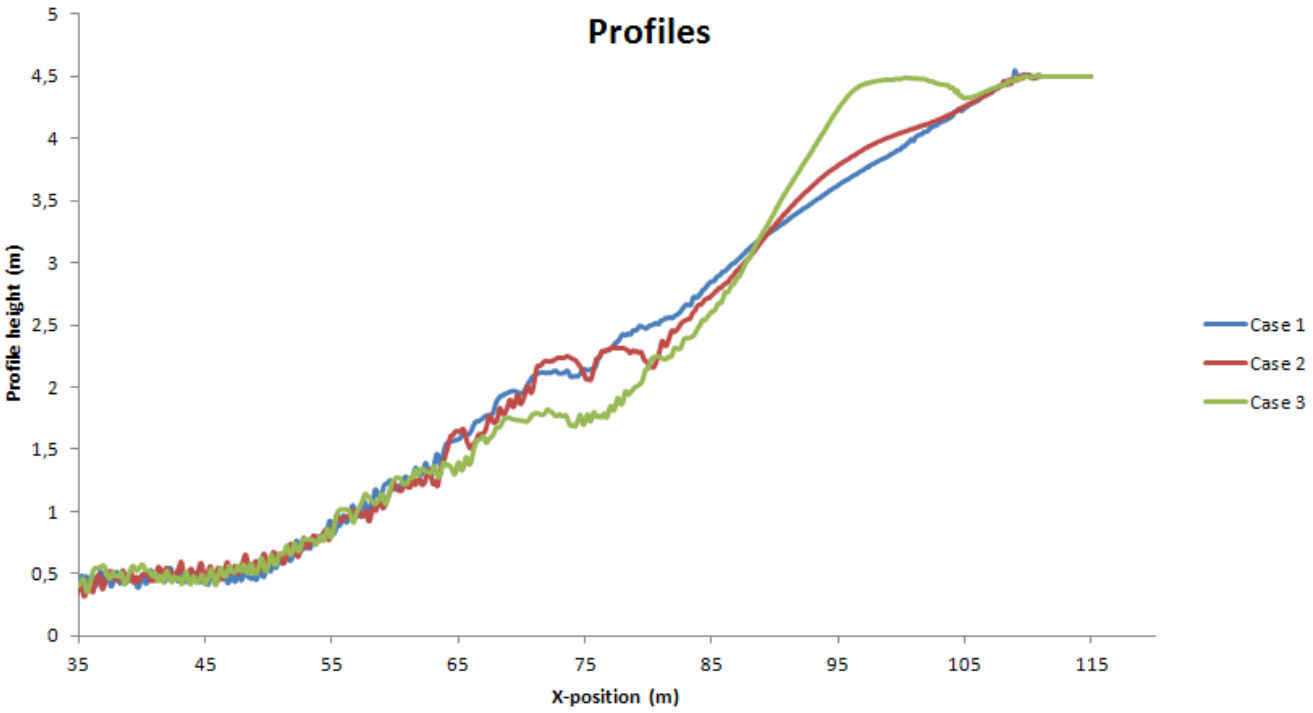

Figure 4.4: Bed profiles for case 1, 2 and 3. Case 1 looks like the initial bed profile. After that the slope becomes steeper, what causes more reflection.

So in summary, the steeper slopes of case 2 and 3 causes more reflection and more noise between two consecutive pressure sensors. That is why the focus in this research will be on case 1, where the reflection is less. From now on, the position of the first pressure (x=36,2 meter) will be placed at an x-position of 0 meter. So in the results the x-axes start with zero, which is the first instrument.

5. Results

5.1 Pressure time series

To get a first insight about the waves in the flume, the sea surface elevation is plotted. In Figures 5.1a, b and c some SSE time series are shown. For these examples, a 30 minutes lasting run from case 1 is chosen and instruments 1, 6 and 10 are shown. Instrument 1 represents the initial situation where waves are mostly symmetrical. Instrument 6 is in the shoaling zone and instrument 10 is in the surf zone where waves are breaking significantly. From these figures it becomes clear that there is indeed a random wave field. Figure 5.1a is the first instrument, where the initial water depth is 3 meter. The significant wave height is 0.8 meter, with a trough at 2.6 meter and a crest at 3.4 meter, however also larger waves (wave height of about 1 meter) and smaller waves in the order of 10-20 centimeters are visible. Instrument 6 and 10 are placed at the slope of the barrier (Figure 4.1), meaning that the mean water depth should be less than 3 meter. This is visible in Figures 5.1b and c. Instrument 6 and 10 have a mean water depth of about 1.5 and 0.75 meter, respectively. The wave pattern looks quite similar with wave heights varying from 0.1 to 1 meter.

Figures 5.1d, e and f show one single wave, belonging to the pressure time series 5.1a, b and c, respectively. Although these waves are chosen somewhat randomly, they give a good overview of the development of waves in deep water, the shoaling and the surf zone. Figure 5.1d is the most symmetrical one of all instruments; however it shows already some properties of a skewed wave. The crest amplitude is 0.5 meter, where the trough amplitude is only 0.25 meter. This means that the first instrument is already in the intermediate zone where the bed affects the waves. Instrument 6 gives an even more skewed wave. There is again a difference in positive and negative amplitude and also the crest duration is larger than the trough duration, so it can be concluded that instrument 6 is fully in the shoaling zone. Instrument 10 (Figure 5.1f) gives an asymmetrical wave, where crest and trough height are equal and where the wave shows the typical saw-tooth shaped form. Apparently instrument 10 is in the surf zone where waves start breaking. These figures are in line with the theory about waves, explained in chapter 2.1 and shown in figure 2.1.1, with the difference that the larger waves are already non-linear at the start in these experiments.

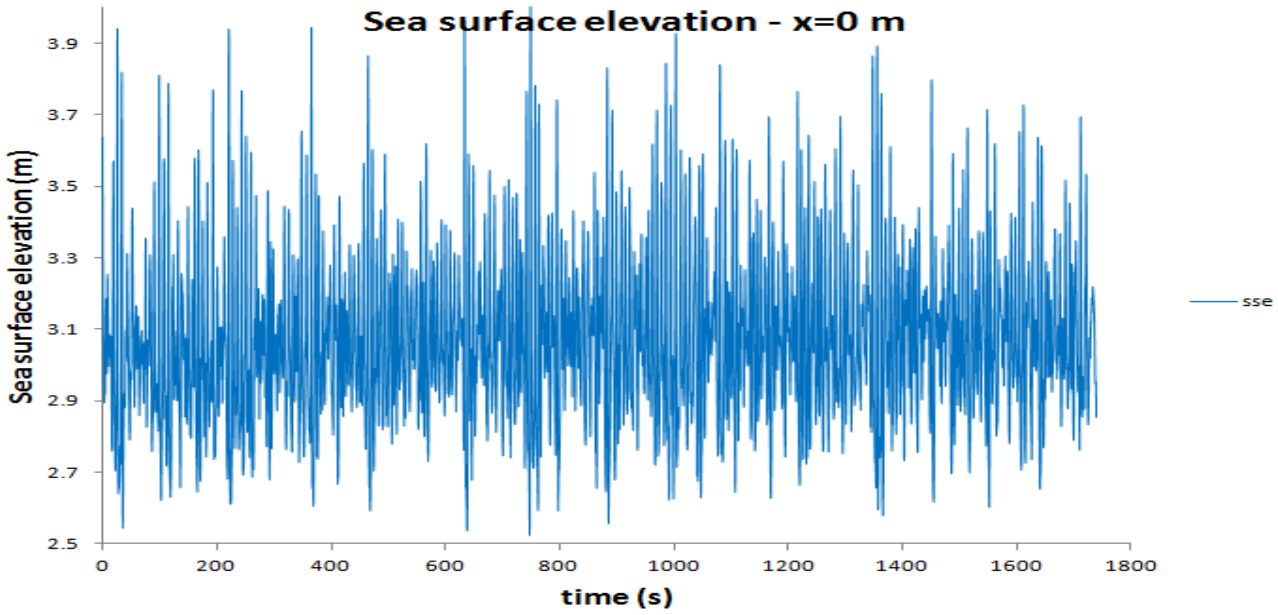

A

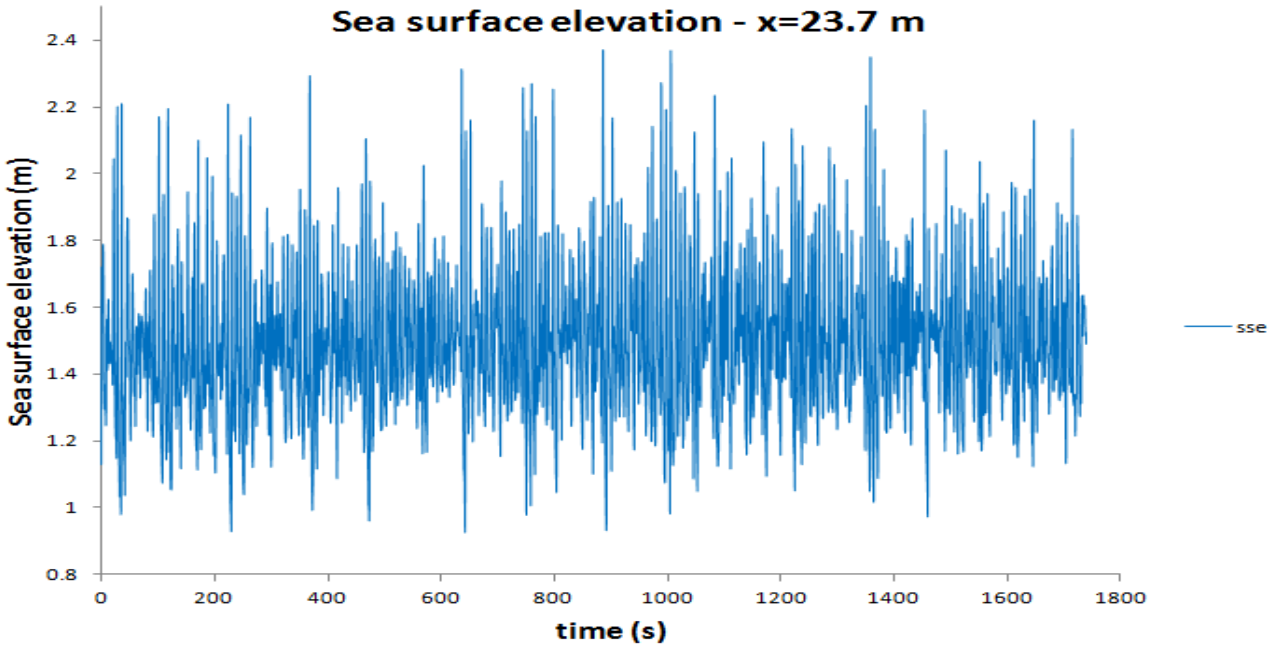

B

Figure 5.1: Pressure time series. For these examples the original run 6 (30 minutes) from case 1 is shown. A, B and C are instruments 1, 6 and 10 respectively. D, e and f show an associated example of one single wave.

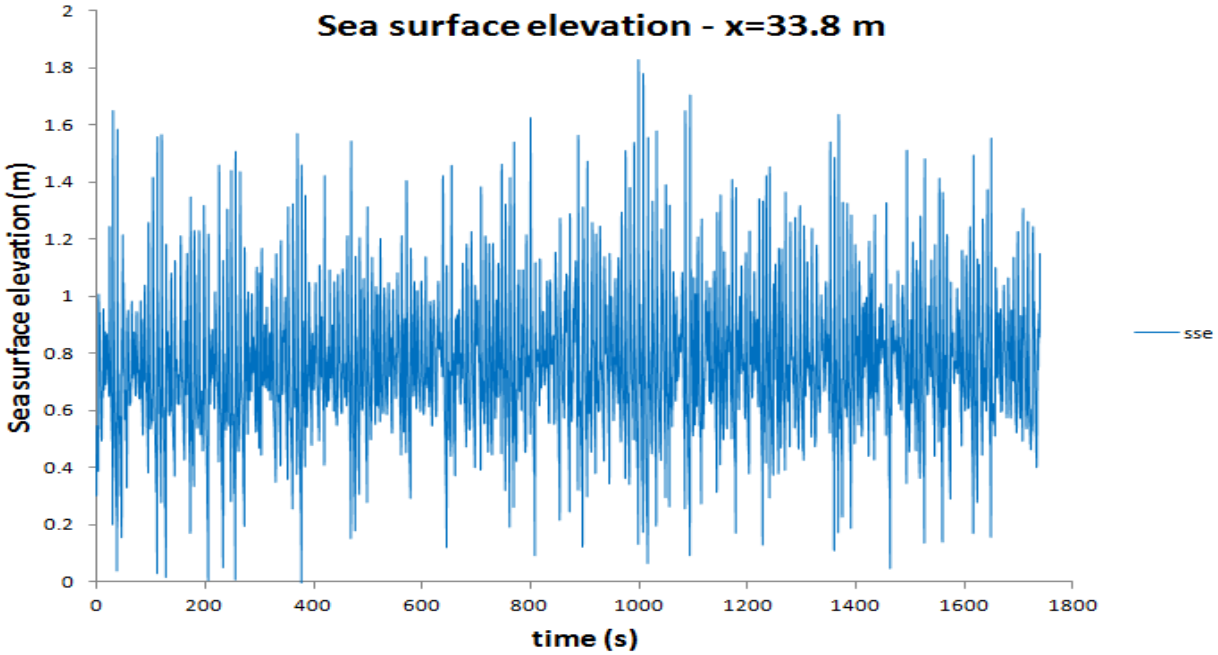

C

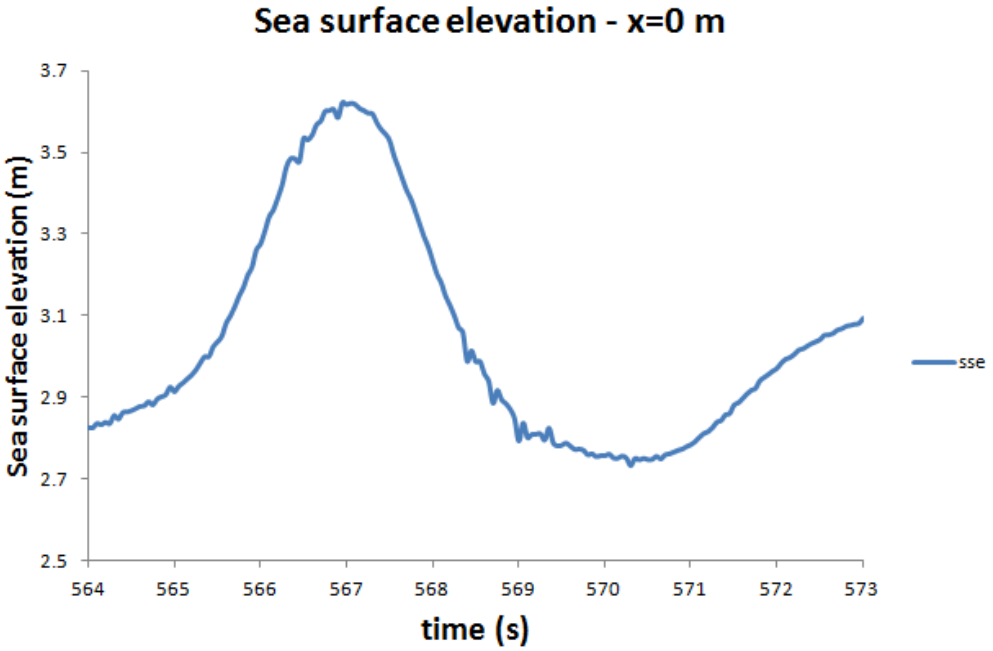

D

Figure 5.1: Pressure time series. For these examples the original run 6 (30 minutes) from case 1 is shown. A, b and c are instruments 1, 6 and 10 respectively. D, e and f show an associated example of one single wave.

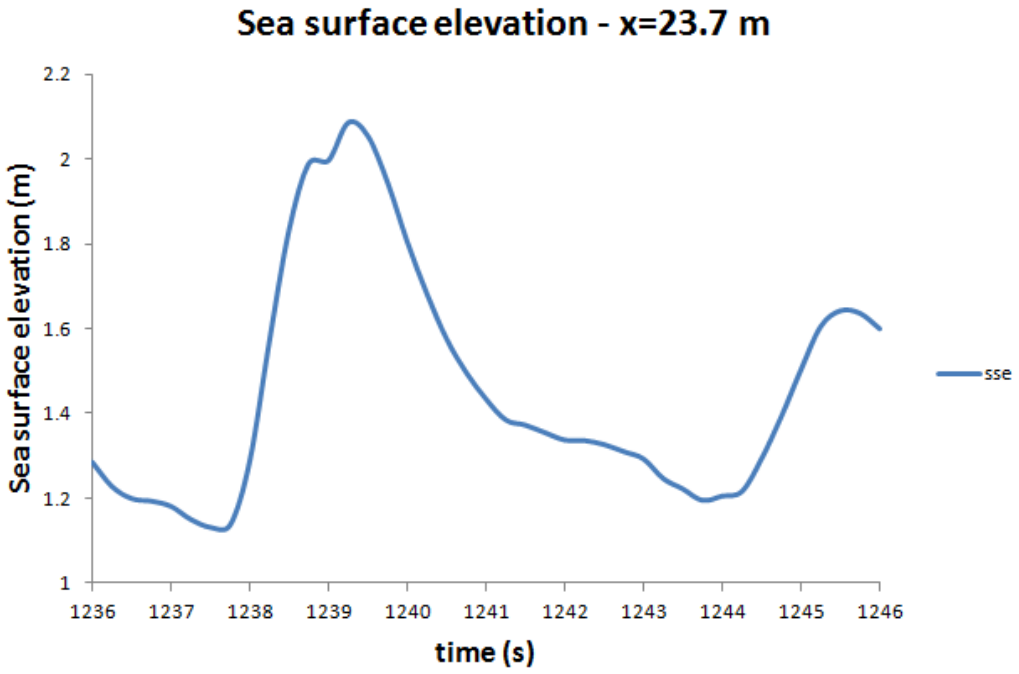

E

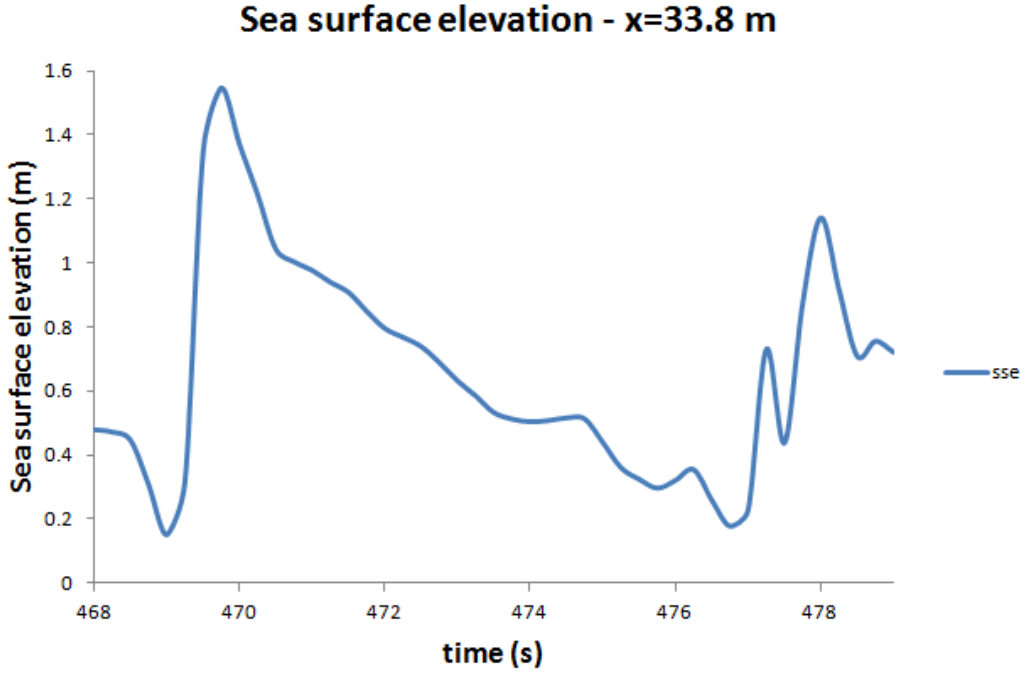

F

Figure 5.1: Pressure time series. For these examples the original run 6 (30 minutes) from case 1 is shown. A, b and c are instruments 1, 6 and 10 respectively. D, e and f show an associated example of one single wave.

5.2 Significant wave height

The development of the wave height is shown in Figure 5.2. Theoretically the wave height should increase in the shoaling zone until waves break, as explained in chapter 2. This is partly the case, as the significant wave height increases from 0.9 to almost 1 meter. However, Figure 5.2 shows that the wave height first goes down. Only from about 25 meter, it increases until the points where waves start breaking. This can have two reasons. Probably these dips are partly caused by reflection. It is also possible that the largest waves of the spectrum break more offshore, which causes the decrease in wave height. It is assumed that wave breaking starts at the position where the wave height is maximal, in case 1 this is at a x-position of 31.2 meter. Case 1 starts with a wave height of 0.9 meter, so apparently the initial significant wave height is 0.9 meter instead of the desired 0.8 meter. It can also be that shoaling caused already an increase in wave height at this offshore position. In the surf zone, the significant wave height decreases quickly to a value of 0.5 meter at the most onshore pressure sensor.

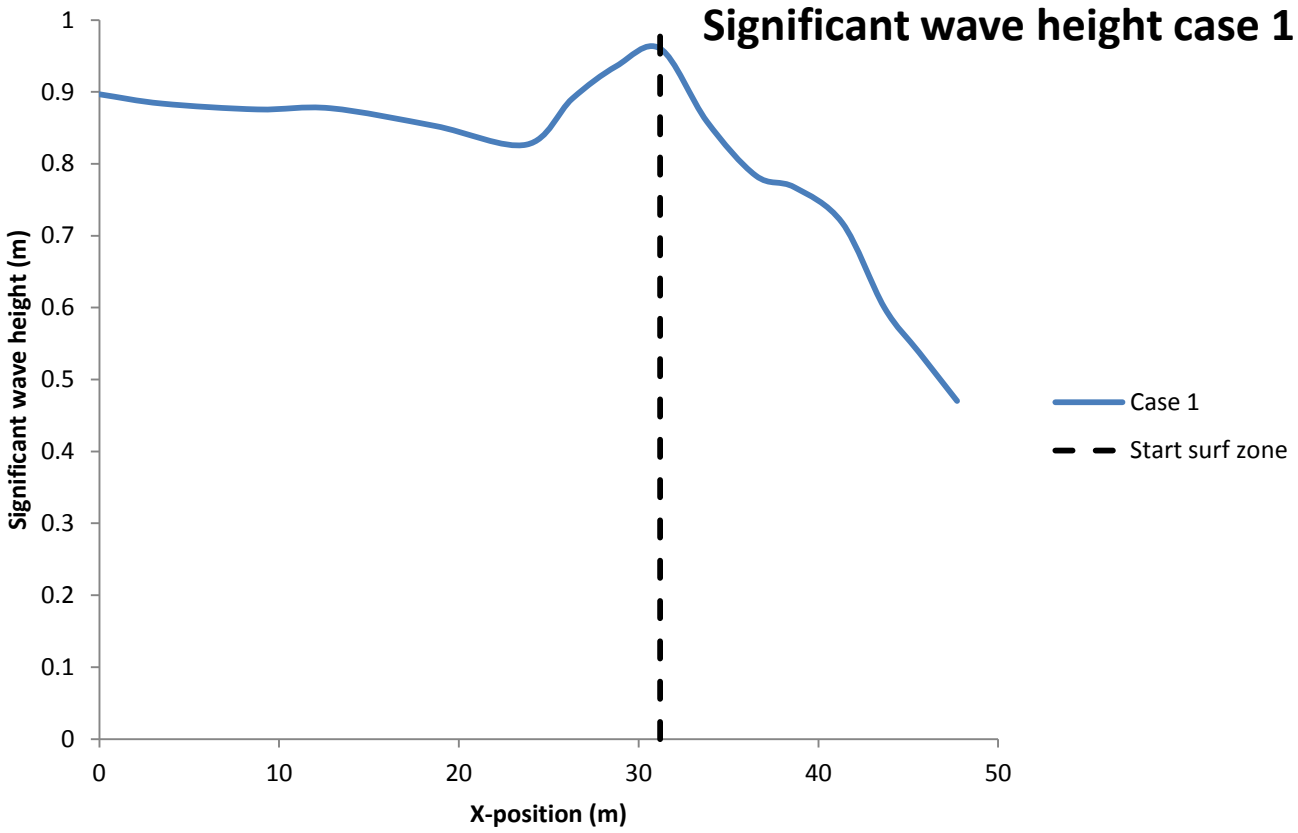

Figure 5.2: Development of wave height in onshore direction. Shoaling of the waves is visible, but there is also a large dip, probably caused by reflection and earlier breaking waves.

5.3 Skewness and asymmetry

Figure 5.3 shows the development of the skewness in onshore direction. In chapter 2.1 it is explained that normally the skewness is maximal at the start of the shoaling zone. This is also the case in these experiments. Case 1 has a skewness value around 1 between 35 and 55 meter, which is quite high.

Figure 5.3 also gives the asymmetry for case 1. It shows the same pattern as described in chapter 2.1. At the start of the shoaling zone, the values are around zero, what means no asymmetry. Then it gradually decreases until the waves start breaking. The asymmetry reaches values of about -1.8, which is again extremely low. This is in line with figure 5.1f, that shows a typical saw-tooth shaped asymmetrical form.

If skewness and asymmetry are researched together, the wave shape development becomes clear. At the start of the shoaling zone waves are skewed and not asymmetrical. Then, in onshore direction, asymmetry is increasing and skewness stays more or less the same. So in this figure the wave development in the shoaling zone from skewed to asymmetrical becomes clear. Also important is that asymmetry values remain quite high in the outer surf zone, so apparently the wave shape stays asymmetrical here.

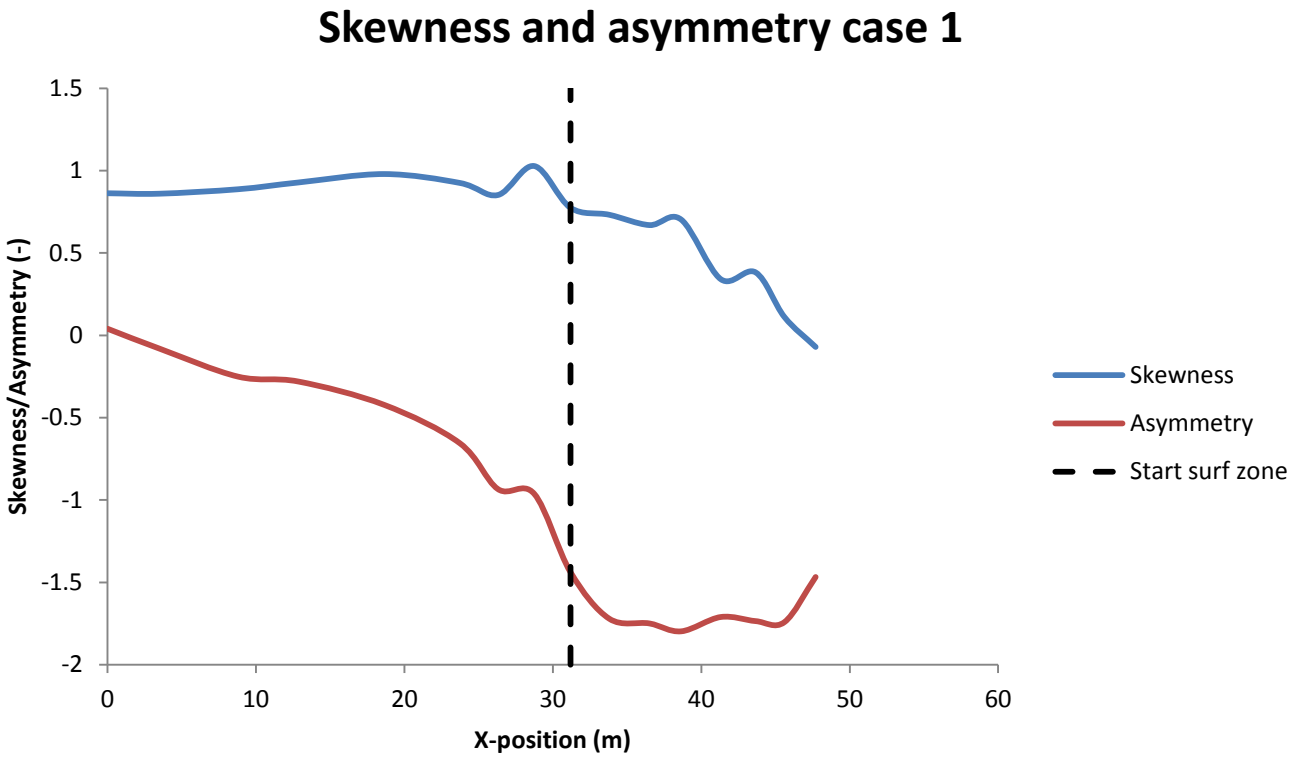

Figure 5.3: Skewness and asymmetry development in onshore direction of all cases. Skewness is maximal at the beginning of the shoaling zone and it decreases in the inner shoaling zone. Asymmetry is zero at the start of the shoaling zone. It becomes larger in onshore direction

5.4 Wave spectrum

5.4.1 Shoaling zone

Figure 5.4 shows three different wave spectra in the shoaling zone of case 1, at the x-position of 0, 18.6 and 31.2 meter. The first one is the furthest offshore instrument and the third one is at the boundary of the shoaling and surf zone. The second spectrum in this figure is somewhere in between. The primary peak is about 0.125 Hz, which is in line with the defined wave period of 8 seconds. Two important properties of these spectra in the shoaling zone are visible.

Firstly, the first harmonic of 0.25 Hz, which is the sum interaction $f_1 + f_1$ (0.25 + 0.25 Hz), is already visible. This secondary peak is one order of magnitude smaller than the primary peak. The presence of the first harmonic is another sign that the first instrument is already in the shoaling zone. There is also a small peak at 0.375 Hz, the second harmonic. This one is likely a result of a sum interaction between the primary and secondary peak ($f_1 + f_2$). The first harmonic of 0.25 Hz remains more or less constant in onshore direction, there is no clear in- or decreasing trend. The small second harmonic of 0.375 Hz becomes more vague in onshore direction. Halfway the shoaling zone this peak is not visible anymore. Instead of this, there is a broader spectral increase in the region 0.3-0.4 Hz. This is in line with the theory about a broad-banded spectrum, as shown by [Norheim et al, 1997], Figure 2.2.5. The spectrum of case 1 is not as broad-banded as the spectrum in Figure 2.2.5, because in Figure 5.4 the first harmonic is visible in a very clear way. However, it is also not as narrow-banded as Figure 2.2.1, where clear higher harmonics arise.

Secondly, the development of the primary peak is slightly different than in the wave spectra of [Norheim et al, 1997]and [Elgar, Guza,1985], explained in chapter 2.2. There the primary peaks go down due to non-linear energy transfers. Here the primary peak is alternately increasing and decreasing in onshore direction instead of only decreasing. Probably this is again caused by reflection, which disturbs the wave signal.

In general, it can be said that the wave spectra in the shoaling zone of case 1 are developing as expected. The first and second harmonics show that there are non-linear wave energy transfers, which cause the wave shape development from linear to skewed to asymmetrical. However, reflection still plays a role in case 1, what becomes clear with the fluctuating primary peak. This must be taken into account in other results.

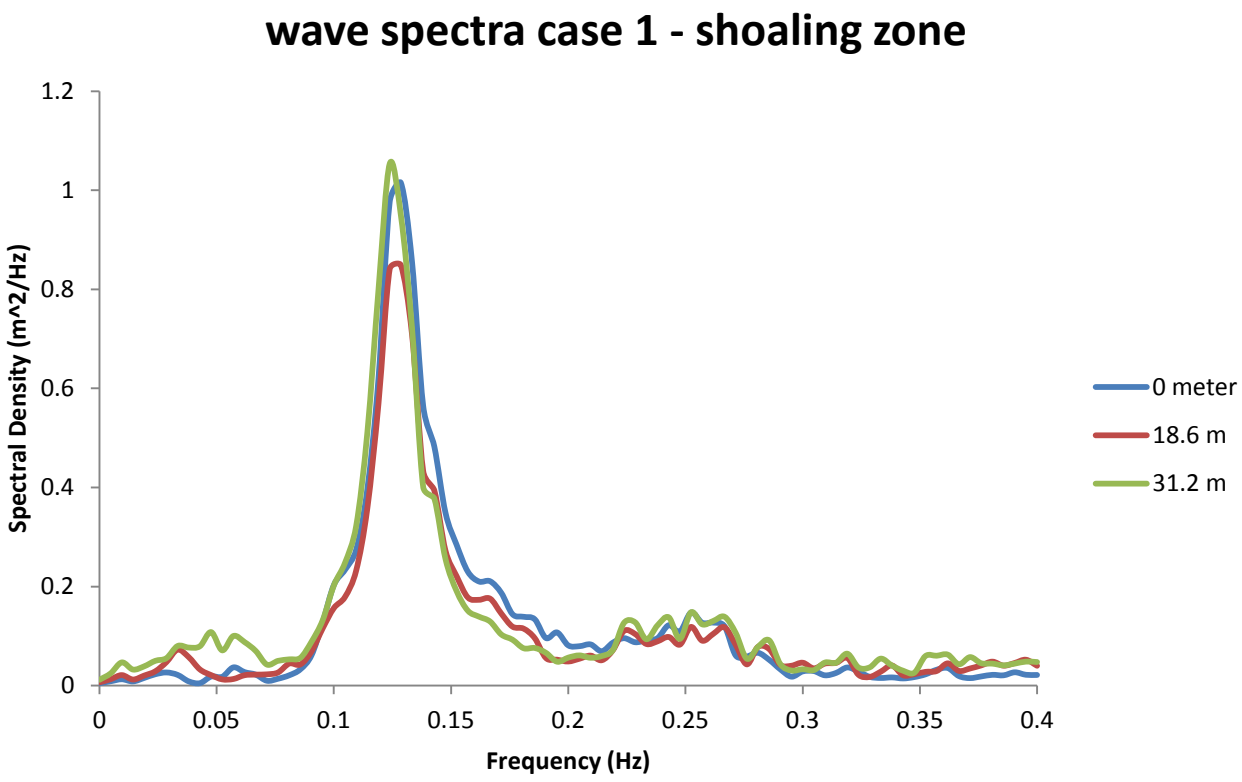

Figure 5.4: Wave spectra of case 1 in the shoaling zone. The first harmonic of 0.25 is visible in a very good way. The primary peak of 0.125 is not decreasing in onshore direction, but fluctuating. This is probably caused by reflection.

5.4.2 Surf zone

Figure 5.5 shows spectra from instruments measuring in the surf zone, at the positions of 31.2, 38.7 and 47.7 meter. 31.2 meter is again the boundary of the shoaling and surf zone, and 47.7 meter is the last and most onshore pressure sensor. Here there are two processes that change the spectra, namely non-linear energy transfers and breaking-related dissipation. With the spectra it cannot be seen which parameter as function of frequency is the most important, but the development of the spectrum as a whole can be described. Firstly, the total energy decreases due to dissipation. This is visible in a clear way, as especially in the higher frequencies the spectrum decreases. The primary peak is visible in all spectra from the surf zone, but it goes down in energy quite fast. The difference in energy of the primary peak between instrument 12 and 16 (38.7 and 47.7 meter) is almost 2 orders of magnitude. The first harmonic decreases in onshore direction as well. In all instruments in the surf zone this secondary peak is visible, but becomes less clear in onshore direction. Also here the total decrease is 2 orders of magnitude. In the frequency region 0.3-0.4 Hz there are no higher harmonics visible anymore. There is only a broad decrease of energy, again with more or less 2 orders of magnitude.

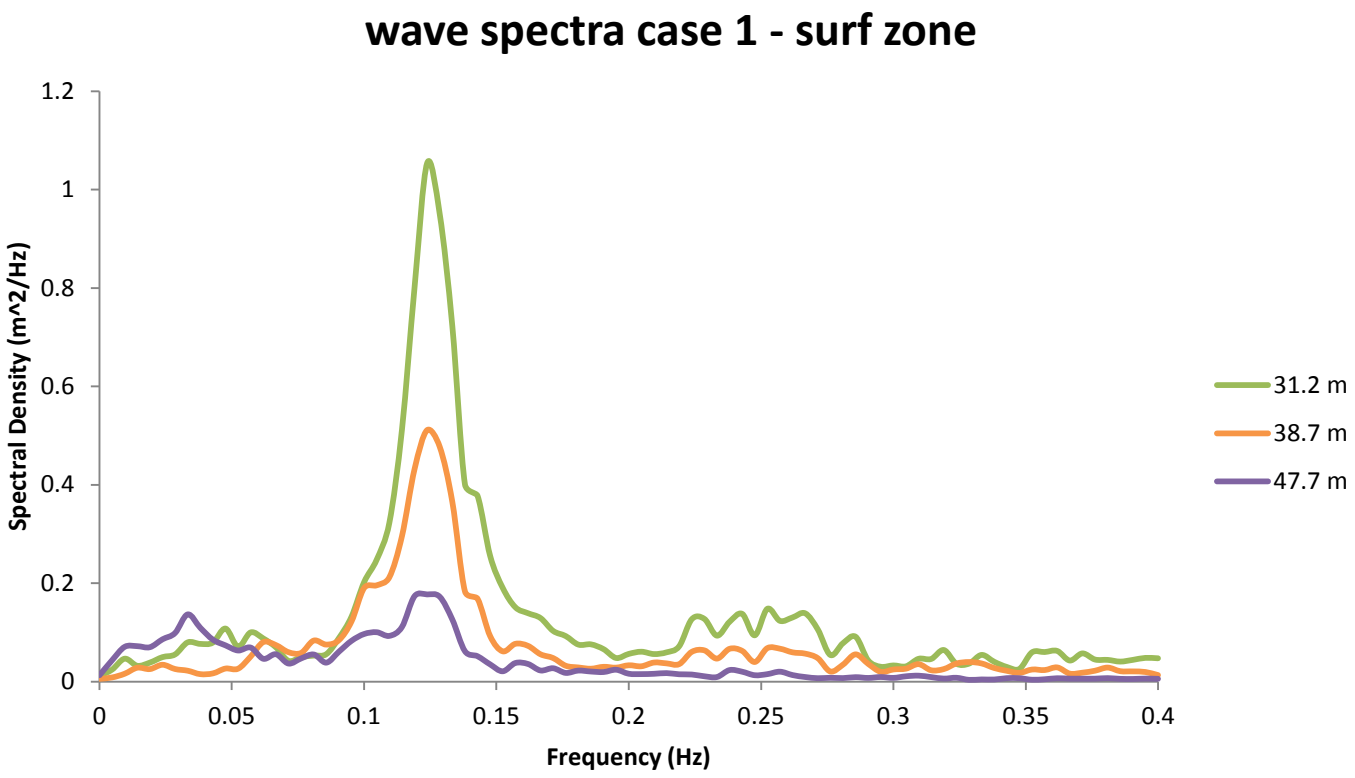

Figure 5.5: Wave spectra of case 1 in the surf zone. An overall decrease of spectra energy in the surf zone is visible in onshore direction. The higher harmonics are disappearing in the surf zone.

5.5 Wave bispectrum

5.5.1 Shoaling zone

Figures 5.6a-e show the wave bispectra of case 1, where 5.6a-c represents the shoaling zone. All bispectra are normalized, in other words the bicoherence is plotted with values between zero (no wave coupling) and one (maximum wave coupling). The bispectra are symmetrical in the diagonal, as for example the wave coupling f_1+f_2 is the same as the wave coupling f_2+f_1. Figure 5.6a shows the first instrument which is closest to deep water. From the sea surface elevation data, the skewness and asymmetry and the wave spectra it was already clear that at the position of this instrument the shoaling zone started already. This is visible once more in this figure. Bicoherence values of 0.65 are present at the wave coupling f_1+f_1 (0.125+0.125 Hz). This wave triad causes the first harmonic shown in Figure 5.4. The wave triads f_1+f_2 (0.125+0.25 Hz) and even f_1+f_3 (0.125+0.375 Hz) are all visible, with bicoherence values of 0.55 and 0.40 respectively. These high values give rise to the conclusion that bispectra are developed very well. The wave triad f_1+f_2 causes the second harmonic of 0.375 Hz. This small peak was indeed visible in Figure 5.4, as mentioned before. The wave coupling of 0.125 and 0.375 Hz causes the third harmonic, however this peak is not visible in the wave spectrum in Figure 5.4. This third harmonic would be 0.50 Hz and this is not plotted, as these values would not be trustworthy anymore.

In the next two bispectra in Figures 5.6b and c, the development of wave triads continues in a clear way. The coupling of two primary waves f_1+f_1 is becoming larger with bicoherence values of 0.75. These values are larger than the values of [Elgar, Guza, 1985], which found values in the trend of 0.50. The other two wave triads shown in Figure 5.6a are still present and bicoherence values are more or less the same. The most striking development is the beginning of the wave triad f_2+f_2 with bicoherence values of 0.40. It contributes together with f_1+f_3 to the third harmonic. Also in the next bispectra in the shoaling zone, the bispectra show more and more wave triads. In Figure 5.6c, just before waves start breaking, even the wave triads f_2+f_3 and f_3+f_3 are visible (bicoherence values in the order of 0.30), which create the fourth and fifth harmonic respectively. Although these peaks are not shown in the spectra of Figure 5.4 due to the fact that these high frequencies are not trustworthy, these bispectra make clear that these peaks certainly exist. It must also be noted that these bispectra give arguments that the spectra of case 1 are narrow-banded, as wave triads are visible at positions where it is expected, creating higher harmonics. Broad-banded spectra would not give such clear spots in the bispectra where wave coupling takes place, but instead give a more vague and broader development of wave coupling.

5.5.2 Surf zone

Figures 5.6d-e show the development of the bispectra in the surf zone, during wave breaking. The development of the secondary peak remains visible until the last instrument in onshore direction, the spot in the bispectra at 0.125 and 0.125 Hz is still there. However, the bicoherence values are decreasing. In the outer surf zone these values are in the order of 0.60, but in the inner surf-zone this is only about 0.35, which is still significant. The same trend is shown for the wave triad f_1+f_2. In the outer surf zone it remains visible, with decreasing bicoherence from 0.55 to 0.30. In the inner surf zone however it becomes harder to distinguish this wave coupling and the wave triad f_1 and f_2, it becomes more a broad picture with wave coupling. This also holds for the development of the third and fourth harmonic. In the shoaling zone these wave triads can be distinguished, but in the surf zone these specific spots in the bispectra disappear. Instead of this there is a broader wave coupling zone with bicoherence between 0.2 and 0.3, which is still significant. This is in line with the wave spectra of case 1 in the surf zone (Figure 5.5), where the higher harmonics disappeared in the surf zone and instead a broader development took place.

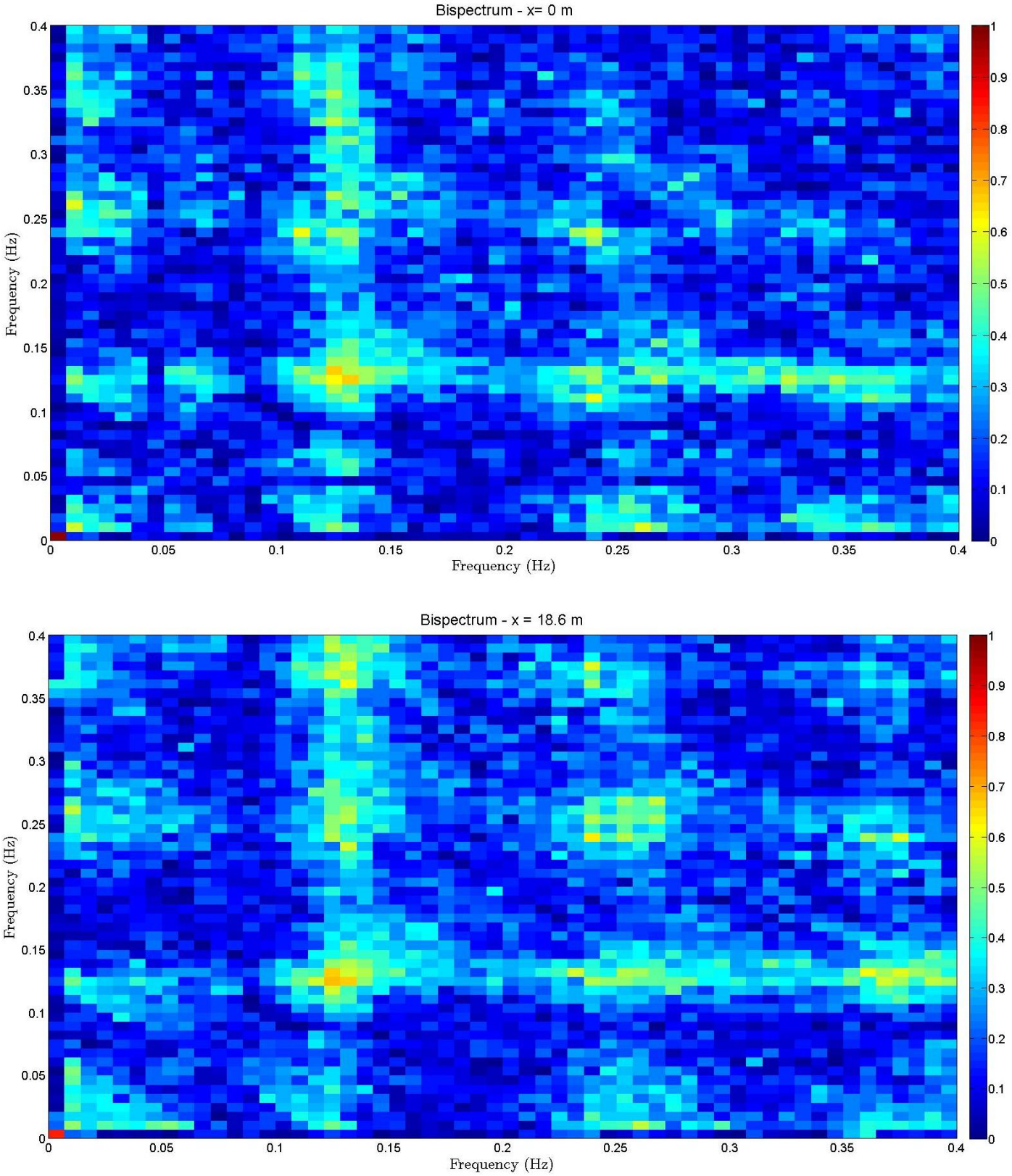

Figure 5.6: Bispectra of case 1. A, B and C are in the shoaling zone and D and E are in the surf zone. In the shoaling zone the bispectral development is clear. In the surf zone, the bicoherence of different wave triads was decreasing.

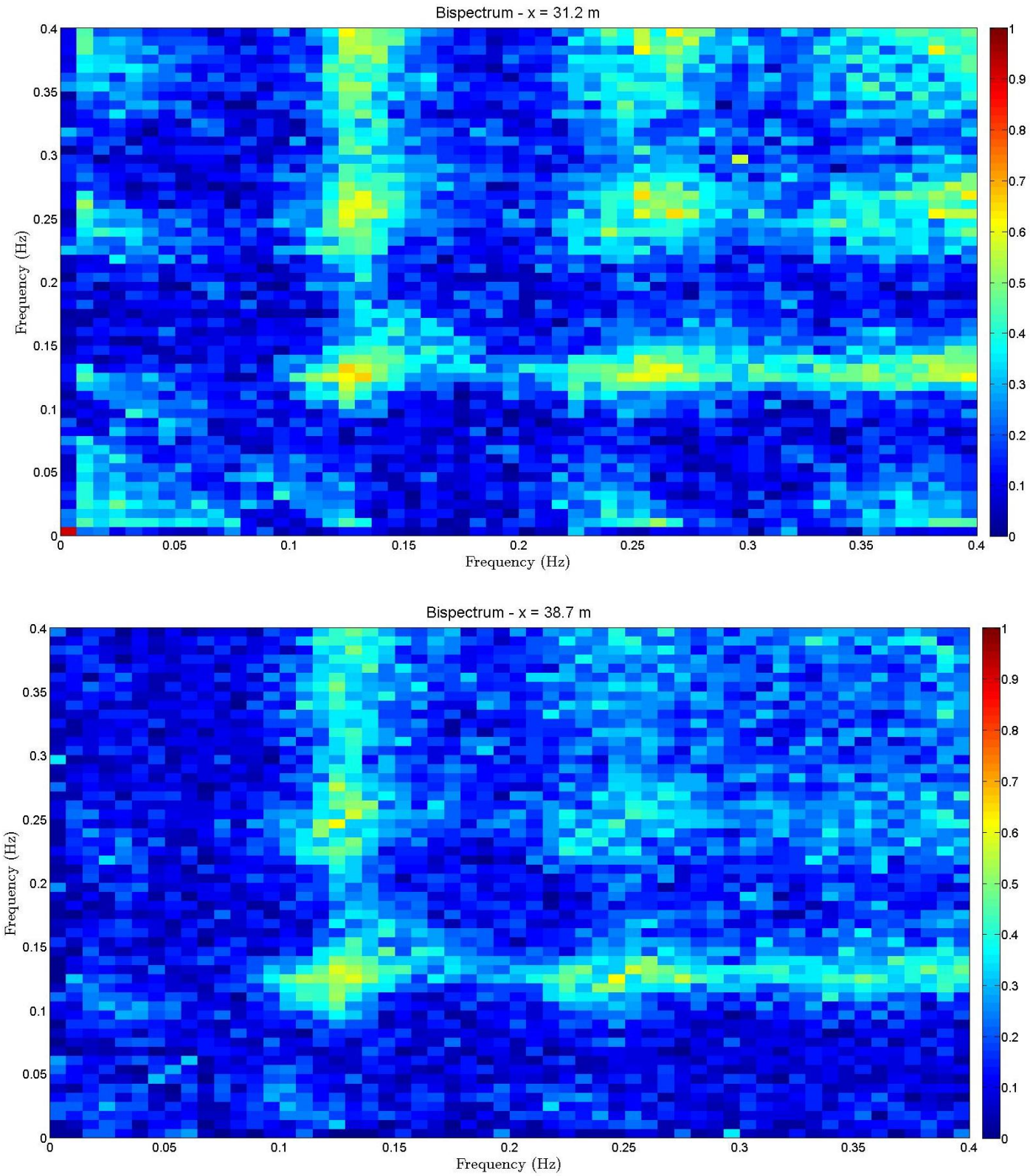

Figure 5.6: Bispectra of case 1. A, B and C are in the shoaling zone and D and E are in the surf zone. In the shoaling zone the bispectral development is clear. In the surf zone, the bicoherence of different wave triads was decreasing.

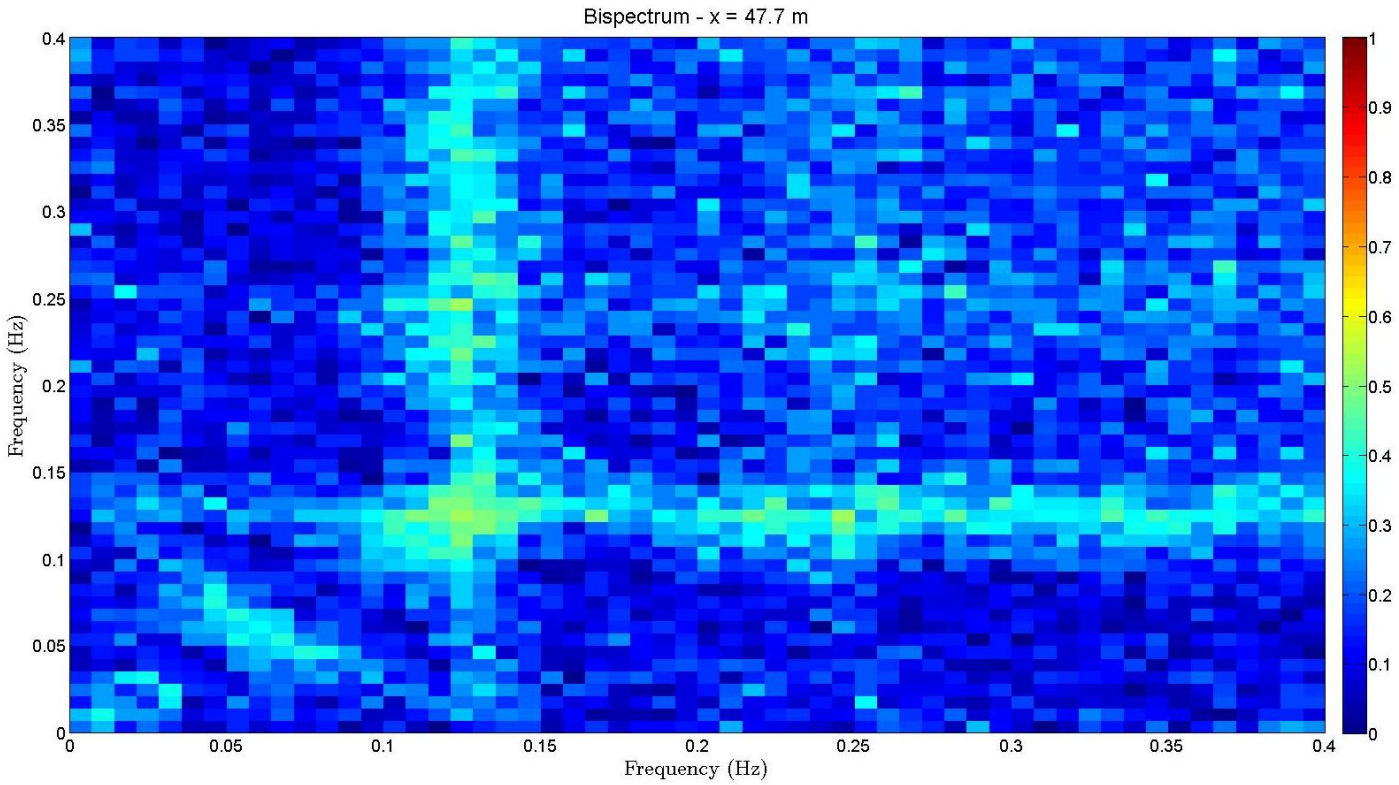

Figure 5.6: Bispectra of case 1. A, B and C are in the shoaling zone and D and E are in the surf zone. In the shoaling zone the bispectral development is clear. In the surf zone, the bicoherence of different wave triads was decreasing.

In Figure 5.7 an overview of the bicoherence development in onshore direction is given for the wave triads f_1+f_1, f_1+f_2, f_2+f_2, and f_1+f_3. It becomes again clear that the first harmonic is already present at the most offshore instrument, as the bicoherence of this wave triad here is in the order of 0.70. Until 12 meter it is increasing and after this point it is slightly decreasing until the start of the surf zone. Here it is decreasing faster to an end value of 0.5. The wave triads f_1+f_2 and f_1+f_3 are also already existing at the start, however the bicoherence is lower (between 0.3 and 0.4). The wave coupling between f_1 and f_2 is higher than the wave coupling between f_1 and f_3 everywhere, which is expected as this wave triad causes the second harmonic instead of the third. Both wave triads increase in bicoherence in onshore direction until the surf zone starts. Then it decreases quite fast. This is in line with the bispectra shown in Figure 5.6, where it becomes clear that wave coupling in the surf zone becomes broader. Furthermore, the wave triad between f_2 and f_2 is also developing in onshore direction. At the start (first instrument), this wave coupling is not significant, but in a later stage in the shoaling zone it increases to values in the order of 0.5. This means that this wave coupling contributes to the third harmonic of 0.5 Hz.

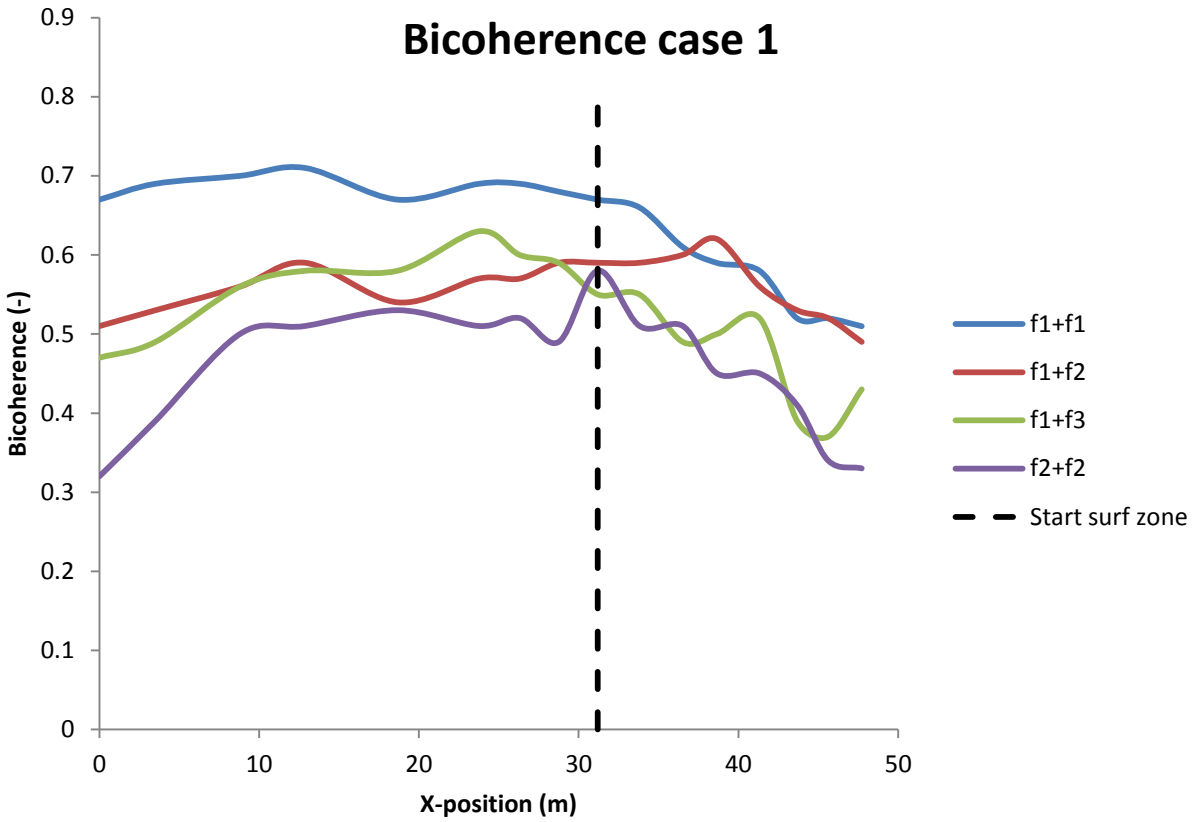

Figure 5.7: Bicoherence in onshore direction of case 1. The four most important wave triads are plotted.

Biphase

Figure 5.8 shows the biphase development in onshore direction in degrees for case 1. In chapter 2.1.3 an explanation about the normal evolution of the biphase between two coupled waves is given, where waves are free in deep water and coupled in the shoaling zone (0 degrees in the outer shoaling zone and -90 degrees in the inner shoaling zone). This is also shown by Figure 2.1.5 by [Elgar, Guza, 1985]. Figure 5.8 shows similar results, where most wave triads behave similarly. At the first instrument the biphase between two coupled waves is between -10 and -30 degrees. This means that waves are already coupled at this point, which is already concluded before. In the remaining part of the shoaling zone the general trend is a decreasing biphase. At 67.5 meter (the end of the shoaling zone) the biphase of the coupled waves is around -60 degrees. This is not the expected -90 degrees as shown in Figure 2.1.5. However, the biphase is still decreasing in the surf zone. At the last instrument the biphase of all plotted wave triads is between -90 and -110 degrees, which is the same as described in chapter 2.1.3. The wave triad f_2+f_2 is slightly different than the others, because at the first instruments the biphase goes from 100 to -100 degrees. The reason could be that these two waves are not coupled yet at this position but act as free waves. This is in line with figure 5.10, where the bicoherence of this wave triad is not significant at the first instruments. At a position of 45 meter, the biphase of this wave triad starts to behave like the others.

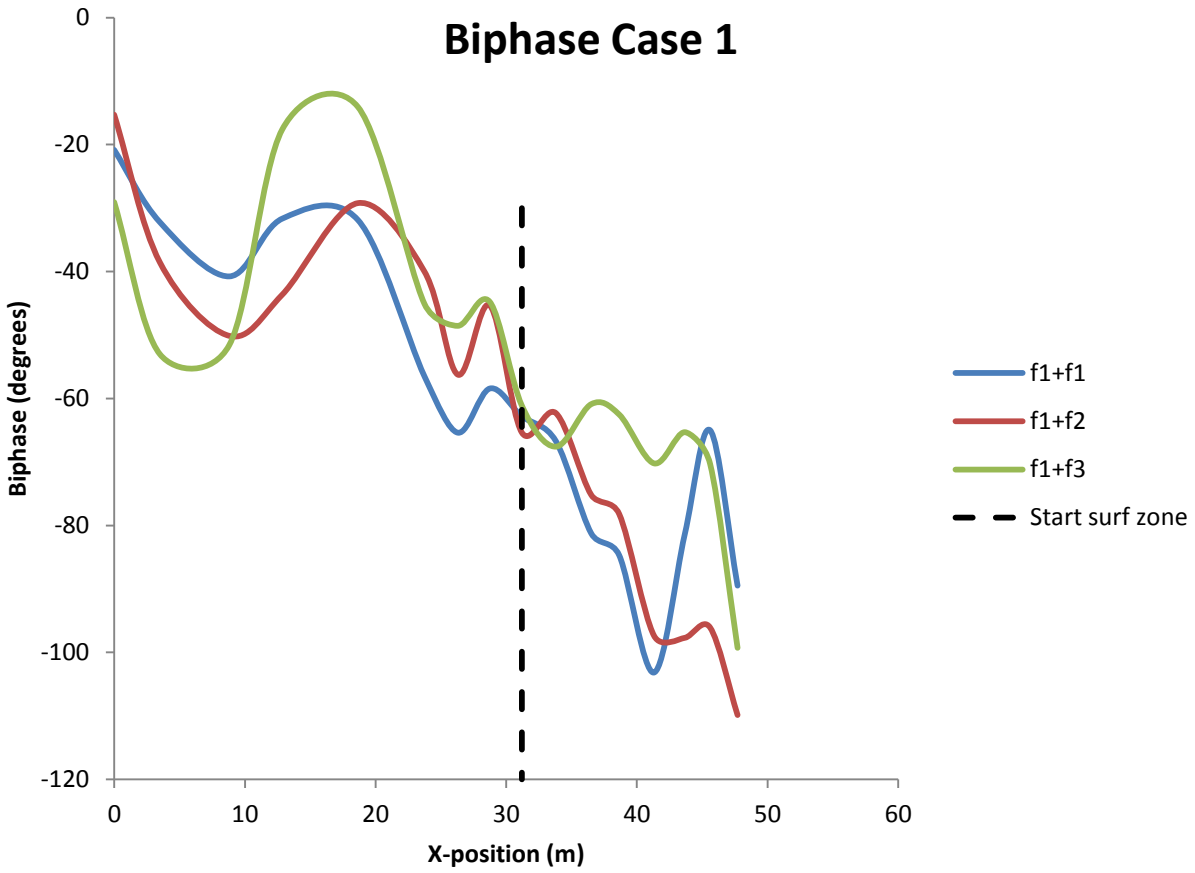

Figure 5.8: The biphase development of case 1. All wave triads show the same trend; 0 degrees at the start of the shoaling zone, -90 degrees at the end of the shoaling zone

5.6 Energy flux and non-linear wave energy transfers

This chapter shows the development of the non-linear wave energy S_{nl} and the energy flux F_x as function of frequency. The difference between these two parameters can be seen as the breaking-related dissipation (S_{ds}). The figures represent positions between two instruments, as F_x is the gradient of energy (the wave spectrum). This means that for example for case 1 there are only 15 figures instead of 16.

5.6.1 Linear wave energy (S_{nl})

Figures 5.9a-e show the development of the non-linear wave energy and energy flux as function of frequency, where 5.9a-c represent the shoaling zone and d-e show the surf zone. A positive S_{nl} means that there is a positive non-linear energy transfer, in other words net energy is received. A negative S_{nl} means that net energy due to non-linear energy transfers is decreasing. At Figure 5.9a S_{nl} is close to zero everywhere, especially compared to the energy flux F_x. However, it is already slightly negative (about -0.2 m^2) around the central peak of 0.125 Hz. This is expected, because chapter 2.2 already showed that the central peak goes down in onshore direction due to wave coupling and non-linear energy transfers. Around the first harmonic of 0.25 Hz a small positive peak of about 0.2 m^2 is visible. This is the result of the wave triad f_1+f_1, which causes an increase of this secondary peak.

These two trends (negative around central peak and positive around first harmonic) continue at the next figures. Figure 5.9b for example shows a S_{nl} of -1 m^2 around the primary peak, which is five times larger than at the first instrument in the outer shoaling zone. This makes clear that non-linear wave energy transfers increase in onshore direction. The positive peak at the first harmonic is still around 0.2 m^2. Figure 5.8c (between instrument 9 and 10, which is the inner shoaling zone) gives an even larger S_{nl} around the primary peak of -8 m^2, almost one order of magnitude larger than Figure 5.8b. Also the peak at the first harmonic is still visible, but then in negative direction (-1 m^2). Apparently the energy loss for example from f_1+f_2 is larger than the energy gain from f_1+f_1. At the second harmonic of 0.375 Hz there is no peak visible in negative or positive direction, but more a general increasing trend with respect to the first harmonic.

Figures 5.8d-e give the development of S_{nl} and F_x in the surf zone. S_{nl} gives the same trends as in the inner shoaling zone. It is negative at the primary peak. At the last figure it is -5 m^2, which is still much larger than at Figures 5.8a-b. Also the negative peak at the first harmonic of -0.5 or -1 m^2 stays constant. Until the plotted 0.4 Hz S_{nl} is completely negative, so apparently the positive non-linear energy takes place in the higher frequencies.

5.6.2 Energy flux (F_x)

The energy flux F_x is in fact the change in spectral energy between two instruments in onshore direction as function of frequency. This means that this F_x should follow the same trend as the wave spectra described in chapter 5.4 and Figure 5.4. The behaviour of F_x around the primary peak tells that this indeed happens. In chapter 5.4 it is explained that this primary peak is alternating instead of going down in onshore direction. Probably this is due to reflection. This is visible as well in Figure 5.8. In Figure 5.8a, the energy flux at the primary peak is negative, but in 5.8b and c this peak is positive. It keeps alternating in the whole shoaling zone. The energy flux in the frequency range 0.2-0.4 is also alternating, but less than the primary peak. In general F_x in this zone is close to zero.

In the surf zone F_x around the primary peak stays negative. Apparently the influence of S_{nl} is larger here than the influence of reflection. This is also shown in the wave spectra of Figure 5.4, where the spectral energy decreases everywhere.

5.6.3 Breaking-related dissipation (S_{ds})

The breaking related dissipation S_{ds} is the difference between S_{nl} and F_x (see equation 2.8). In the shoaling zone this should be zero, as there is no wave breaking in this zone. In other words, S_{nl} and F_x should be equal. However, reflection prevents that this is the case. In the frequency range 0.2-0.4 the two parameters are more or less the same, but around the primary peak it is different. Here F_x fluctuates between positive and negative and S_{nl} is always negative. It is more interesting to look at the dissipation in the surf zone, as wave breaking must be taken into account here. Here the negative peaks of the two parameters at the primary peak have the same order of magnitude, so that it can be concluded that dissipation here is zero. There are still some differences due to reflection (both parameters are alternately larger), but the trend is quite clear. In the higher frequency range F_x is more negative than S_{nl}. In other words, total spectral energy decrease cannot be explained completely by non-linear energy transfers, but also dissipation takes place here.

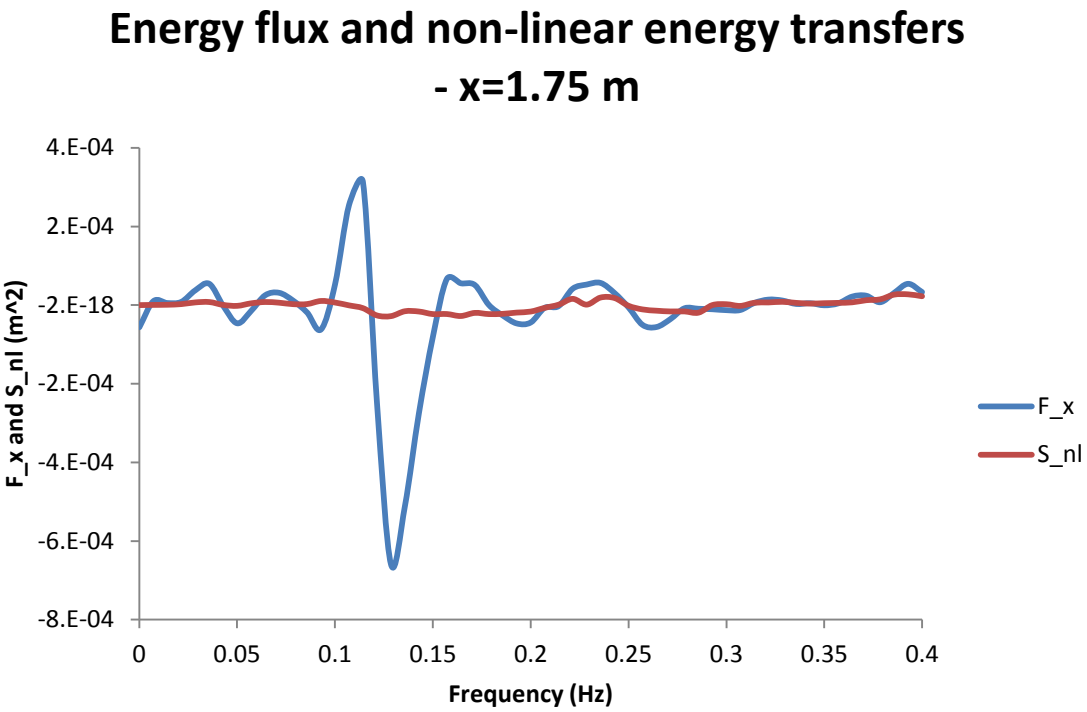

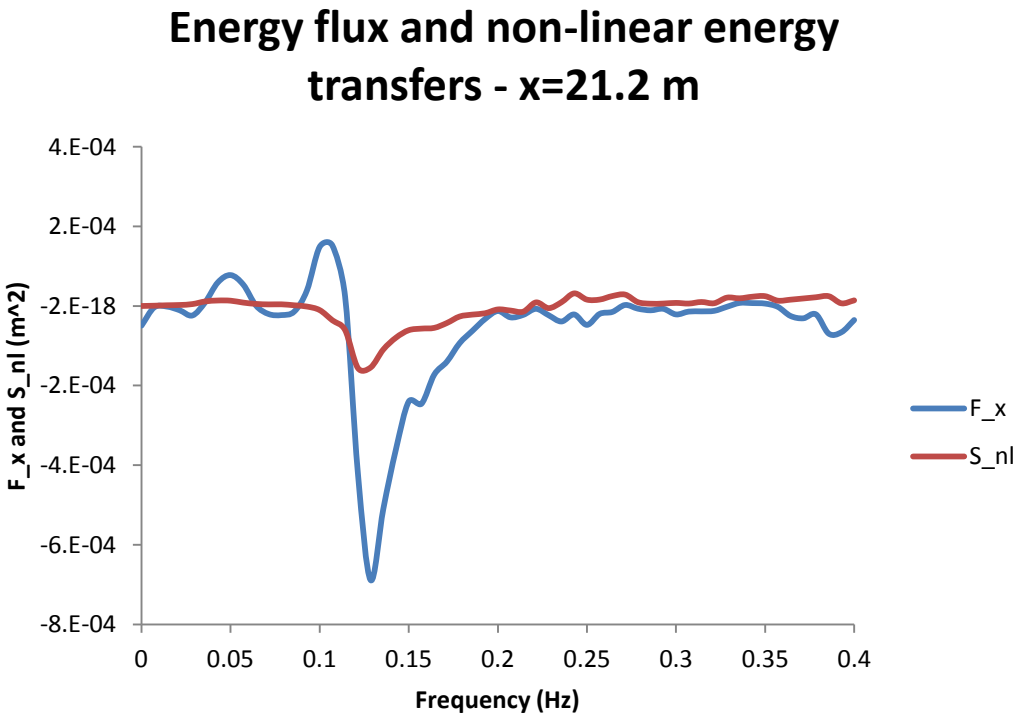

Figure 5.9: The energy flux gradient (F_x) and the nonlinear energy transfer term (S_nl). The difference is the breaking related dissipation (S_ds). Figures a-c represent the shoaling zone, d and e are in the suf zone.

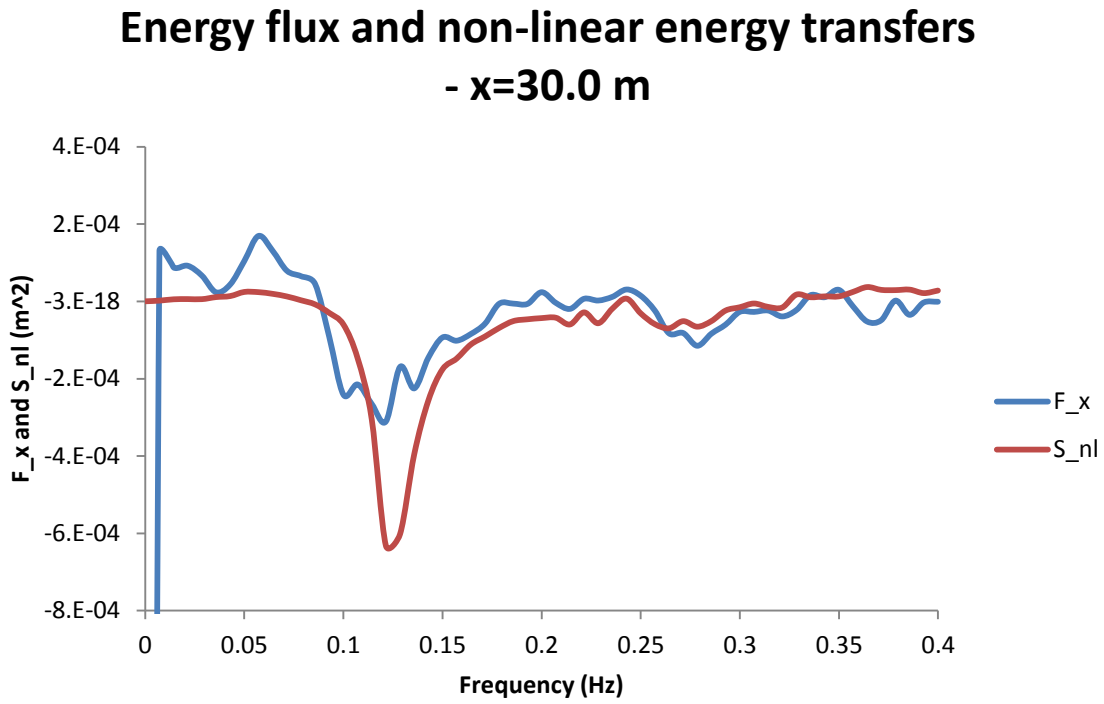

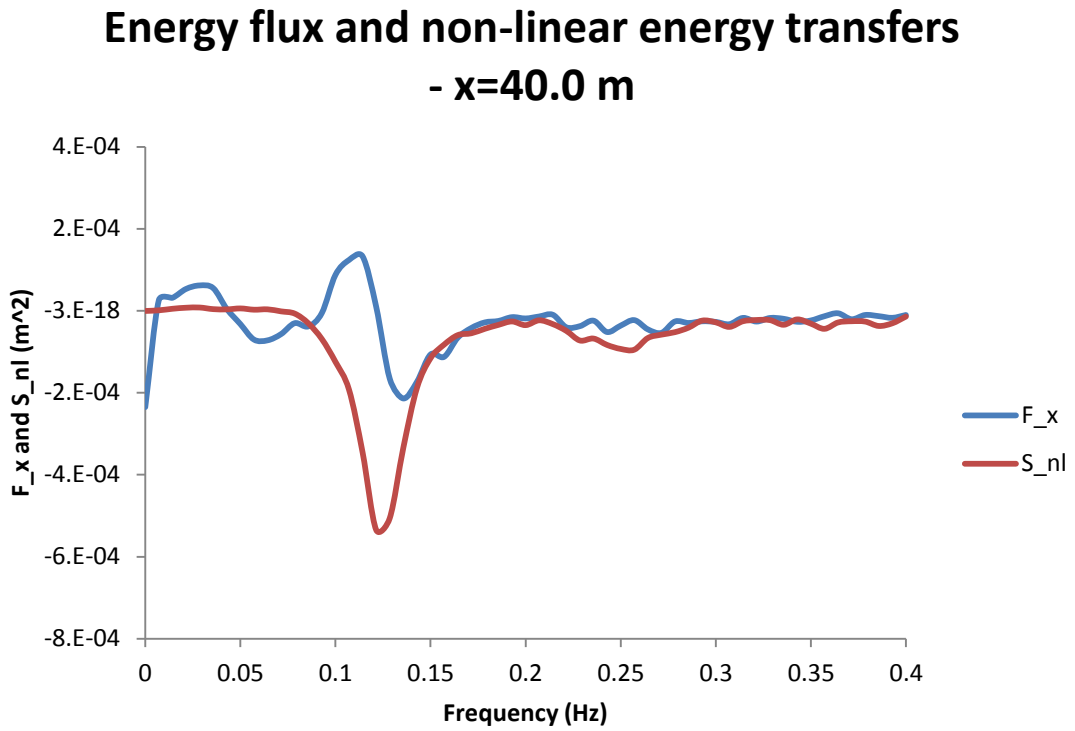

Figure 5.9: The energy flux gradient (F_x) and the nonlinear energy transfer term (S_nl). The difference is the breaking related dissipation (S_ds). Figures a-c represent the shoaling zone, d and e are in the suf zone.

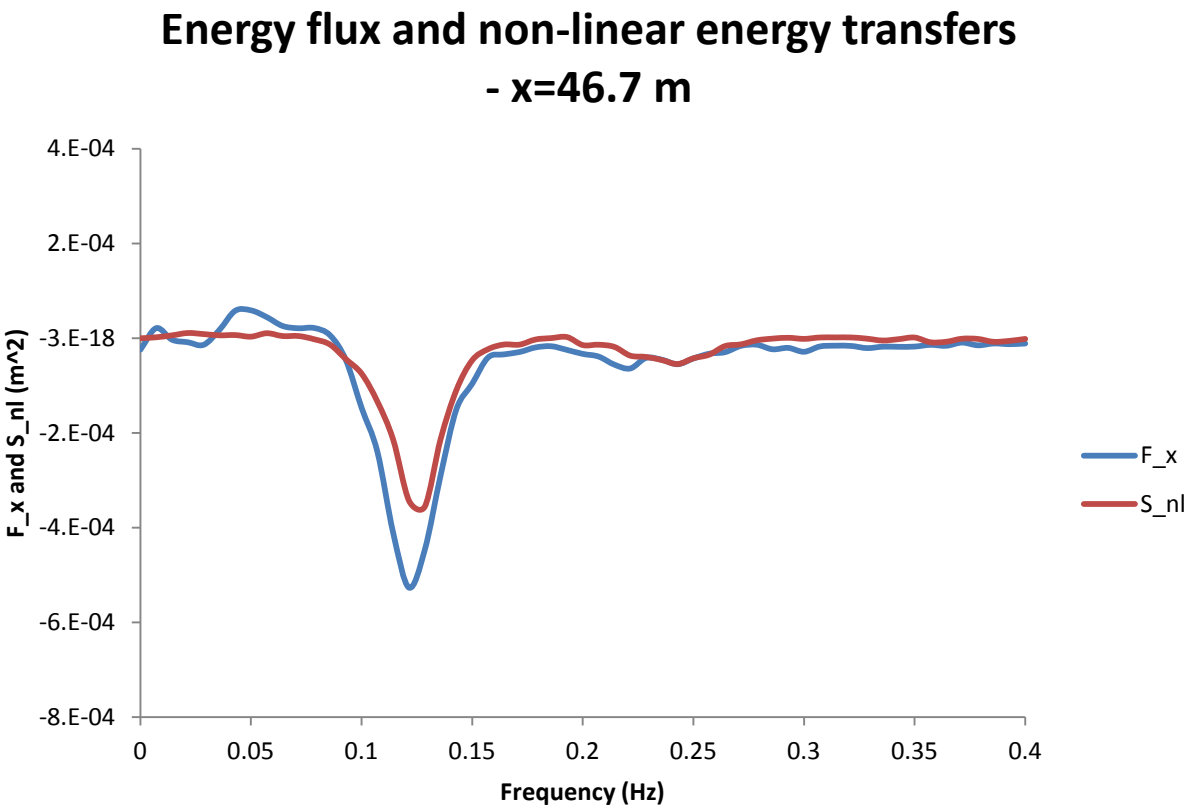

Figure 5.9: The energy flux gradient (F_x) and the nonlinear energy transfer term (S_nl). The difference is the breaking related dissipation (S_ds). Figures a-c represent the shoaling zone, d and e are in the suf zone.

5.7 Relative Dissipation

Figure 5.10 shows the relative dissipation of one position in the surf zone of case 1 (that is dissipation divided by spectral energy) as function of frequency. This figure is shown in order to check the theory of [Kuznetsov, Saprykina, 2004], which tells that the dissipation trend depends on the position in the surf zone. These figures are comparable with figure 2.3.1 from [Elgar et al, 1997]. The results in chapter 5.6 of case 1 show that there is no dissipation in the lower frequency range (0-0.2 Hz) but that dissipation exists in the higher frequency range (0.2-0.4 Hz). Therefore it would be interesting to research whether there are relative dissipation-trends in this zone, comparable with figure 2.3.1. There is plotted only one figure at one position, because al positions in the surf zone showed exactly the same trend. In the second part of the spectrum at the higher frequency range, a horizontal relation is found. However, the reliability of this result is not very clear. For example, sometimes the relative dissipation is even negative, which is not possible. So no linear or squared trend in this second part of the spectrum is found.

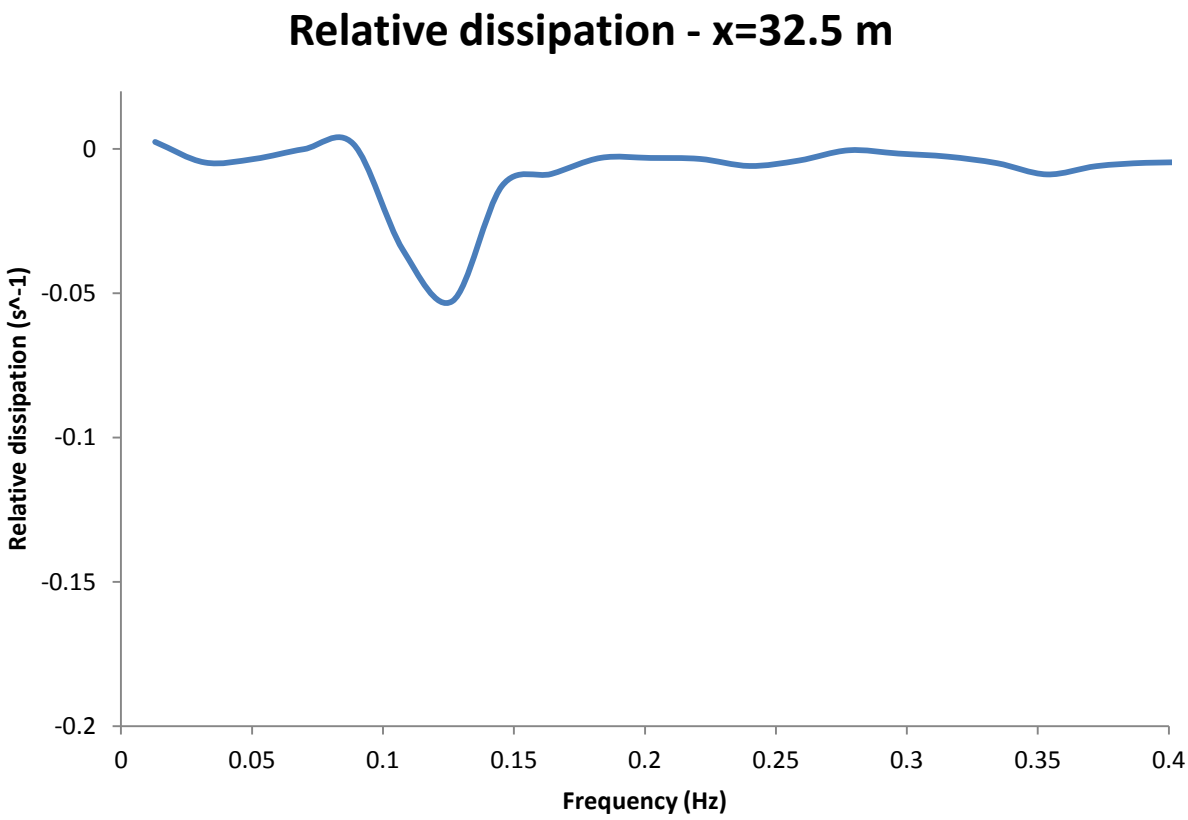

Figure 5.10: The relative dissipation in the surf zone of case 1. A horizontal trend is found in the higher frequency range (0.2 – 0.4 Hz). The reliability of this result is questionable.

6. Discussion

The main goal of this paper was to research the role of wave breaking-related dissipation on the spectral and bispectral evolution in the surf zone. In more detail, a relation between frequency and relative dissipation (dissipation divided by spectral energy) was not fully understood yet. Furthermore, 3 cases were performed with variation in wave height, wave period and water level, to see possible differences in the aforementioned questions. For this goal, three theories were outlined in chapter 2.3, which were found in the literature. These theories state that relative dissipation depends on frequency squared, relative dissipation is equal for every frequency range and dissipation only exists in the higher frequency range respectively. Besides, a combination between theory 1 and 2 states that in the outer surf zone theory 2 holds, while in the inner zone dissipation depends on frequency squared (theory 1).

With analyzing the results, reflection was ignored. However, morphology change during the experiments caused a steeper slope of the barrier, which generated significant reflection. For this reason, there is focused on case 1, because here the barrier slope was still close to the initial slope.

The experiments that were performed in the Delta Flume in the Noordoostpolder were on real scale in a highly controlled environment. It is important to check the general and expected wave, spectral and bispectral properties in the shoaling zone, because then it is known whether waves in this flume behaved like real sea-waves or not, and whether this waves in the shoaling zone followed the expected trend as been visible in many experiments and field works. It was expected that waves developed in a natural way, as these waves were on real scale. When waves in a flume are much smaller, there could be scale-influences. Therefore this discussion first goes into detail about the results in the shoaling zone. Then the results in the surf zone will be discussed, and the research questions will be answered.

6.1 Shoaling zone

The overall trend in the shoaling zone for the development of the significant wave height was increasing in onshore direction, which is caused by the process of shoaling (energy remains constant, but wave speed decreases due to lower water level). This wave shoaling was visible in the wave spectra as well as in the bispectra. All spectra in the shoaling zone, which started already at the first pressure measuring instrument, showed a primary peak equal to the significant wave frequency. Furthermore, the first harmonic of two times the wave period of the primary peak was visible clearly. This first harmonic is not part of the JONSWAP spectrum, so this is an indication that wave coupling took place and the expected wave triads (in this case f_1+f_1) existed. Also the bispectra in the shoaling zone were comparable with the bispectra from literature as explained in chapter 2.2. Wave coupling mainly occurred between the primary peak and its higher harmonics. Further onshore, more higher harmonics were visible, until even the wave triad f_2+f_3, which causes the fourth harmonic, appeared. Also bicoherence values were very high, sometimes the wave triad f_1+f_1 gave values of more than 0.7.

There were more signs that waves developed in a natural way. For example, the skewness and asymmetry almost perfectly followed the trend as explained in chapter 2.1. Skewness was maximum at the start of the shoaling zone, which is the most seaward instrument with values around 1. Closer to the surf zone, skewness slightly decreased. Asymmetry was very close to zero at the start of the shoaling zone. This follows the natural wave development, where waves are first skewed and become more

asymmetrical in the onshore direction. In these experiments, asymmetry values close to the surf zone were in the order of -1.8, which is very low, which means a very high asymmetry. Also the biphase, which controls the degree of skewness and asymmetry, developed in onshore direction. At the start of the shoaling zone, values were around zero degrees. This means that waves were already coupled here and that they were highly skewed. In the onshore direction, the biphase slowly evolved to values around -90 degrees, indicating asymmetrical waves. Furthermore, the development of the non-linear energy transfers developed in an expected way. At the start of the shoaling zone this S_{nl} was negative around the primary peak, what means that it gives energy to the higher harmonics. Around the first harmonic S_{nl} was positive in the shoaling zone, so it received energy from the primary peak. In contrast to the bispectra, only the first harmonic was visible here. However, the results showed that values above 0.35 Hz were not really reliable, so that could be the reason.

However, there were also signs that the waves were not developing in a complete natural way and without other, unwanted processes. For example, for all cases a dip was shown in the significant wave height in onshore direction. This dip was for all cases more or less between x-positions of 45 and 60 meter. The same kind of an unexpected process was visible in the wave spectra. Due to non-linear wave energy transfers, the primary peak should decrease in onshore direction, so that the higher harmonics could increase. However, this primary peak was not consequently going down, but it was alternating. Sometimes the peak was even 50% higher than the primary peak at the start of the shoaling zone. This was also visible in the energy flux parameter (F_x), because it is related to the spectral energy in a direct way. These processes were probably caused by reflection. When the results in the surf zone are researched, this role of reflection must be kept in mind.

In summary, several results show that waves were developing in a natural and expected way. However, reflection (even in case 1) caused some unexpected results, which must be kept in mind when the results in the surf zone are researched.

6.2 Surf zone

The spectral energy in the surf zone decreased at all frequency ranges. A total decrease is expected, due to wave breaking-related dissipation. Besides, the order of magnitude was the same everywhere. For example, case 1 showed that between instrument 9 (just before the start of the surf zone) and instrument 16 (the most shoreward) the whole spectrum was decreasing with more or less two orders of magnitude. This is in line with theory 2, which states that the shape of the spectra remains the same and that there is a horizontal relation between relative dissipation and frequency. However, the role of non-linear wave transfers in the surf zone is not taken into account here; this theory assumes that this does not exist. The bispectra from the surf zone showed that this idea is wrong. The clear spots around the primary peak and its higher harmonics with the very high bicoherence values gradually disappeared, but still a broad wave coupling with significant bicoherence values was visible. Also the development of S_{nl} as function of frequency showed that this theory cannot be correct. These non-linear wave energy transfers around the primary peak were maximum (negative) just before the surf zone. In the surf zone it was becoming smaller, but still significant high values remained. Therefore it can be concluded that the spectral change in the surf zone is not only due to dissipation, but also due to non-linear wave energy transfers.

With this in mind, theory 3 (no dissipation in the lower frequency range) could be researched, which is done at the same way as [Herbers et al, 2000]. This means that the wave flux F_x and the non-linear energy S_{nl} were plotted in the same figure. The difference between them should then be the dissipation S_{ds}. As already explained, F_x was fluctuating around the primary peak, probably due to reflection. This makes it somewhat complicated to compare these two terms with each other in a qualitative way. However, it can be said that in case 1 the order of magnitude of both terms in the lower frequency range (0-0.2 Hz) was the same. Where F_x was alternately higher and smaller, S_{nl} is quite constant. The fact that these terms were more or less equal in the lower frequency range, means that there is no dissipation here. In the higher frequency range (0.2-0.4), S_{nl} was consequently higher (less negative) than F_x. This difference is caused by dissipation. So for case 1 it can be concluded that theory 3 (only dissipation in the higher frequency range) is correct.

Until now, it can be concluded that theory 3 explains the role of frequency on dissipation, where there is no dissipation in the lower frequency range. However, theory 3 can be extended by finding a relation between relative dissipation and frequency in the higher frequency range (0.2 – 0.4 Hz). For this part of the spectrum, there could be a horizontal relation, or it could be that here the relative dissipation is dependent on frequency squared. However, a horizontal relation for this part of the spectrum was found. This would mean that (only for the high frequency range) theory 2 is correct. However, it is not sure whether this result is correct. Firstly, the data were less reliable in this part of the spectrum, and moreover, the dissipation was sometimes even negative, which is not possible. More research about this is necessary.

In summary, it can be said that theory 3 is right. For the zone where dissipation existed, a horizontal trend was found, but more research about this part of the spectrum is needed.

7. Conclusion

The research question was to find the role of wave breaking on the development of wave spectra and bispectra in the surf zone, with the ultimate aim to elucidate the relation between relative dissipation and frequency. Besides, three cases with variable wave height, wave period and water level were performed in order to see any possible differences with different wave properties.

For this goal, three theories that came from literature were outlined that describe the role of frequency on breaking-related dissipation. These theories were tested with real-scale experiments in the Delta Flume. It seemed that theory 3, which states that dissipation only occurs in the higher frequency range (0.2-0.4 Hz), is correct. This means that in the lower frequency range, spectral energy is only decreasing due to non-linear wave energy transfers.

Also an attempt was done to extend theory 3 and to find a trend in the higher frequency range, where dissipation occurs. A horizontal trend was found, however, more research is needed to find a relation between relative dissipation and frequency in this higher frequency range.

References

Beji S. and Battjes J.A., 1993; Experimental investigation of wave propagation over a bar; Coastal engineering; vol. 19, 151-162

Collis W.B., White P.R., Hammond J.K., 1998; Higher order spectra: The bispectrum and trispectrum; Mechanical systems and signal processing; vol. 12(3), 375-394

Eldeberky Y. and Battjes A., 1996; Spectral modeling of wave breaking: Application to Boussinesq equations; Journal of geophysical research; vol. 101, 1253-1264

Elgar S. and Guza R.T., 1985; Observations of bispectra of shoaling surface gravity waves; Journal of fluid mechanics; vol. 161, 425-448

Elgar S., Guza R.T., Raubenheimer B., Herbers T.H.C. and Gallagher E.L., 1997; Spectral evolution of shoaling and breaking waves on a barred beach; Journal of geophysical research; vol. 102, 15797-15805

Hamm L., Madsen P.A. and Howell Peregrine D., 1993; Wave transformation in the nearshore zone: a review; Coastal Engineering; vol. 21, 5-39

Herbers T.H.C., Russnogle N.R. and Elgar S., 2000; Spectral energy balance of breaking waves within the surf zone; Journal of physical oceanography; vol. 30, 2723-2737

Kuznetsov S.Yu. and Saprykina Ya.V., 2004; Frequency-dependent energy dissipation of irregular breaking waves; Water resources; vol. 31, 384-392

Mansard E.P.D. and Funke E.R., 1980: The measurement of incident and reflected spectra using a least squares method; Coastal engineering; part 1: Theoretical and observed wave characteristics; 154-172

Masselink G. and Hughes M.G., 2003: Introduction to coastal processes & geomorphology

Norheim C.A., Herbers T.H.C. and Elgar S., 1998; Nonlinear evolution of surface wave spectra on a beach; Journal of physical oceanography; vol. 28, 1534-1551